EUROPEAN ORGANIZATION FOR NUCLEAR RESEARCH (CERN)

CERN-EP-2017-218
2018/10/11

CMS-HIN-15-008

Pseudorapidity and transverse momentum dependence of flow harmonics in pPb and PbPb collisions

The CMS Collaboration*

Abstract

Measurements of azimuthal angular correlations are presented for high-multiplicity pPb collisions at $\sqrt{s_{_{\mathrm{NN}}}} = 5.02\,\mathrm{TeV}$ and peripheral PbPb collisions at $\sqrt{s_{_{\mathrm{NN}}}} = 2.76\,\mathrm{TeV}$. The data used in this work were collected with the CMS detector at the CERN LHC. Fourier coefficients as functions of transverse momentum and pseudorapidity are studied using the scalar product method, 4-, 6-, and 8-particle cumulants, and the Lee–Yang zeros technique. The influence of event plane decorrelation is evaluated using the scalar product method and found to account for most of the observed pseudorapidity dependence.

Published in Physical Review C as doi:10.1103/PhysRevC.98.044902.

*See Appendix A for the list of collaboration members

1 Introduction

High energy density matter with quark and gluon degrees of freedom, a state of matter known as the quark-gluon plasma (QGP), is created in relativistic heavy ion collisions at the BNL RHIC and at the CERN LHC [1–6]. The energy density created in the initial heavy ion collision is azimuthally nonuniform as a consequence of the collision geometry and its fluctuations. Interactions among constituents in the QGP convert this nonuniformity into an observable anisotropy in the final-state particle momentum distribution. The azimuthal angle distribution of emitted particles can be characterized by its Fourier components [7]. In particular, the second and third Fourier components, v_2 and v_3, known as elliptic and triangular flow, respectively, most directly reflect the medium response to the initial collision geometry and its fluctuations [8]. The magnitudes of these components provide insights into the fundamental transport properties of the medium [9–11]. Two-particle correlations in the azimuthal angle (ϕ) and pseudorapidity (η) differences between the two particles ($\Delta\phi$ and $\Delta\eta$) have played a vital role in the observation of the azimuthal anisotropies [12–19]. These particle correlations are characterized by a pronounced structure at $|\Delta\phi| \approx 0$ extending over a large $\Delta\eta$ range (referred to as the "ridge"). In collisions between two heavy nuclei, such as CuCu and AuAu collisions at RHIC [12–14] and PbPb collisions at the LHC [16–19], these long-range correlations are often attributed to the collective flow from a strongly interacting, expanding medium [20, 21]. This is corroborated by multiparticle correlations, suggesting a hydrodynamic origin for the observed azimuthal anisotropies [22].

The lightest systems in which ridge-like structures have been observed include high-multiplicity final states in pp [23–27] and pPb [27–32] collisions at the LHC. Evidence of such long-range correlations is also observed at a nucleon-nucleon center-of-mass energy of $\sqrt{s_{_{\mathrm{NN}}}} = 200\,\mathrm{GeV}$ in pAu [33], dAu [34–36] and ^{3}HeAu collisions [37] at RHIC. In pPb collisions, the overall strength of the correlation is observed so far to be significantly larger than in pp collisions, and is comparable to that found in peripheral PbPb collisions [38, 39].

Both the ATLAS [40, 41] and CMS [38] experiments have measured significant elliptic flow coefficients in pPb collisions at $\sqrt{s_{_{\mathrm{NN}}}} = 5.02\,\mathrm{TeV}$ using four-particle correlations based on the cumulant method [42]. The long-range correlations persist in measurements that study the correlation among six or more particles in pPb collisions [26, 39, 43] and in measurements of four-particle and six-particle correlations in pp collisions at $\sqrt{s} = 13\,\mathrm{TeV}$ [26, 41]. Four-particle correlation measurements in the dAu system at $\sqrt{s_{_{\mathrm{NN}}}} = 200$, 62.5, 39, and 19.6 GeV by the PHENIX Collaboration and a six-particle correlation measurement by the same collaboration at $\sqrt{s_{_{\mathrm{NN}}}} = 200\,\mathrm{GeV}$ also find significant elliptic flow coefficients [44].

In combination, these measurements support a collective origin of the azimuthal correlations, and have raised the possibility that a QGP droplet might be formed in small-system collisions exhibiting fluid-like behavior [28–30, 39, 45]. If such a mechanism can be confirmed, it will significantly extend the range of system size for which the QGP medium is considered to exist. However, the origin of the ridge phenomenon in small collision systems is still being actively investigated. In addition to a hydrodynamic origin [45, 46], possible alternative explanations include gluon saturation in the initial interacting state of the protons [47, 48], multiparton interactions [49], and the anisotropic escape of partons from the surface of the interaction region [50].

To provide further constraints on the theoretical understanding of the azimuthal anisotropies in different collision systems, this paper presents results on the pseudorapidity and transverse momentum dependence of the flow harmonics in pPb and PbPb collisions. The v_2 coefficients are measured using the 4-, 6-, and 8-particle Q-cumulants [51], the Lee–Yang zeros (LYZ) [52], and the scalar product methods [53, 54]. The v_3 coefficients, which result from fluctuations in the collision geometry, are studied with the scalar product method. Within the hydrodynamic picture, the longer lifetime of the medium on the Pb-going side in pPb collisions is expected to lead to larger values for both the v_2 and v_3 flow harmonics than on the p-going side [55]. The pPb system is studied at $\sqrt{s_{_{\rm NN}}} = 5.02$ TeV using data obtained by the CMS experiment in 2013. A sample of PbPb collision data at $\sqrt{s_{_{\rm NN}}} = 2.76$ TeV is also analyzed. The particle correlations are studied for high-multiplicity pPb collisions whose particle densities are comparable to those in mid-central (50–60% centrality) PbPb collisions. The centrality variable is defined as a fraction of the inelastic hadronic cross section in heavy ion collisions, with 0% corresponding to the most central, i.e., head-on collisions. This allows for a direct comparison of pPb and PbPb systems over a broad range of similar particle multiplicities, thereby helping to clarify the underlying mechanism responsible for the observed correlations.

2 The CMS experiment

A detailed description of the CMS detector can be found in Ref. [56]. The results in this paper are mainly based on the silicon tracker detector and two hadron forward calorimeters (HF) located on either side of the tracker. Situated inside the 3.8 T field of a super-conducting solenoid, the silicon tracker consists of 1 440 silicon pixel and 15 148 silicon strip detector modules. It measures charged particles within the range of $|\eta| < 2.4$ and provides an impact parameter resolution of $\approx$15 μm and a $p_{\rm T}$ resolution better than 1.5% at $p_{\rm T} \approx 100$ GeV/c. Electromagnetic (ECAL) and hadron (HCAL) calorimeters are also located inside the solenoid and cover the range of $|\eta| < 3.0$. The HCAL has sampling calorimeters composed of brass and scintillator plates. The ECAL consists of lead-tungstate crystals arranged in a quasi-projective geometry. Iron/quartz-fiber Cherenkov HF cover the range $2.9 < |\eta| < 5.2$ on either side of the interaction region. The HF calorimeters, which are used in the scalar product analysis, are azimuthally subdivided into 20° modular wedges and further segmented to form $0.175 \times 10°$ $(\Delta\eta \times \Delta\phi)$ towers. The CMS detector response is determined through Monte Carlo (MC) studies using GEANT4 [57].

3 Event and track selection

The pPb data set corresponds to an integrated luminosity of 35 nb^{-1}. The beam energies were 4 TeV for protons and 1.58 TeV per nucleon for lead nuclei, resulting in $\sqrt{s_{_{\rm NN}}} = 5.02$ TeV. The beam directions were reversed during the run. The results from both beam directions are combined using the convention that the proton-going direction defines positive pseudorapdity. As a result of the energy difference between the colliding beams, the nucleon-nucleon center-of-mass frame in the pPb collisions is not at rest with respect to the laboratory frame. Massless particles emitted at $\eta_{\rm c.m.} = 0$ in the nucleon-nucleon center-of-mass frame will be detected at $\eta = 0.465$ in the laboratory frame. Unless otherwise stated, all pseudorapidities reported in this paper are referred to with respect to the laboratory frame. A sample of $\sqrt{s_{_{\rm NN}}} = 2.76$ TeV PbPb data collected during the 2011 LHC heavy ion run, corresponding to an integrated luminosity of 2.3 μb^{-1}, is also analyzed for comparison purposes. The triggers, event selection, and track reconstruction are identical to those used in Ref. [38].

In order to select high-multiplicity pPb collisions, dedicated high-multiplicity triggers were implemented using the CMS level-1 and high-level trigger (HLT) systems. The online track reconstruction at the HLT is based on the three layers of pixel detectors, and requires a track origin within a cylindrical region of length 30 cm along the beam axis and radius 0.2 cm perpendicular to the beam axis, centered at the nominal interaction point. For each event, the vertex reconstructed with the highest number of pixel tracks is selected. The number of pixel tracks ($N_{\text{trk}}^{\text{online}}$) with $|\eta| < 2.4$, $p_{\text{T}} > 0.4\,\text{GeV}/c$, and a distance of closest approach to this vertex of 0.4 cm or less, is determined for each event. Several high-multiplicity ranges are defined with prescale factors that are progressively reduced until, for the highest multiplicity events, no prescaling was applied.

In the offline analysis, hadronic collisions are selected by requiring a coincidence of at least one HF tower containing more than 3 GeV of total energy on either side of the interaction region. Only towers within $3.0 < |\eta| < 5.0$ are used in order to avoid the edges of the HF acceptance. The pPb interactions were simulated with both the EPOS LHC [58] and the HIJING 1.383 [59] event generators. The requirement of having at least one primary particle with total energy $E > 3.0\,\text{GeV}$ in each of the η ranges $-5.0 < \eta < -3.0$ and $3.0 < \eta < 5.0$ is found to select 97–98% of the total inelastic hadronic cross section.

Events in the offline analysis are also required to contain at least one reconstructed primary vertex within 15 cm of the nominal interaction point along the beam axis (z_{vtx}) and within 0.15 cm transverse to the beam trajectory. At least two reconstructed tracks are required to be associated with the primary vertex. Beam-related background is suppressed by rejecting events for which less than 25% of all reconstructed tracks pass the track selection criteria for this analysis. The pPb instantaneous luminosity provided by the LHC in 2013 resulted in an approximately 3% probability of at least one additional interaction occurring in the same bunch crossing. Such pileup events become more significant as the event multiplicity increases. Following the procedure developed in Ref. [38] for rejecting pileup events, a 99.8% purity of single-interaction events is achieved for the pPb collisions belonging to the highest multiplicity class of this analysis.

The CMS "high-quality" tracks described in Ref. [60] are used in this analysis. Additionally, a reconstructed track is only considered as a candidate track from the primary vertex if the significance of the separation along the beam axis (z) between the track and the best vertex, $d_z/\sigma(d_z)$, and the significance of the track impact parameter measured transverse to the beam, $d_{\text{T}}/\sigma(d_{\text{T}})$, are each less than 3. The relative uncertainty in p_{T}, $\sigma(p_{\text{T}})/p_{\text{T}}$, is required to be less than 10%. To ensure high tracking efficiency and to reduce the rate of incorrectly reconstructed tracks, only tracks within $|\eta| < 2.4$ and with $p_{\text{T}} > 0.3\,\text{GeV}/c$ are used in the analysis. The entire pPb data set is divided into classes of reconstructed track multiplicity, $N_{\text{trk}}^{\text{offline}}$, where primary tracks with $|\eta| < 2.4$ and $p_{\text{T}} > 0.4\,\text{GeV}/c$ are counted. A different p_{T} cutoff of $0.4\,\text{GeV}/c$ is used in the multiplicity determination because of the constraints on the online processing time for the HLT. The multiplicity classification in this analysis is identical to that used in Ref. [38], where more details are provided, including a table relating $N_{\text{trk}}^{\text{offline}}$ to the fraction of minimum bias triggered events.

The peripheral PbPb data collected during the 2011 LHC heavy ion run with a minimum bias trigger are also reanalyzed in order to compare directly the pPb and PbPb systems in the same $N_{\text{trk}}^{\text{offline}}$ ranges [38]. This PbPb sample is reprocessed using the same event selection and track reconstruction as for the present pPb analysis. A description of the 2011 PbPb data set can be found in Ref. [61]. The correspondence between the PbPb $N_{\text{trk}}^{\text{offline}}$ values and the total energy deposited in the HF [62], as characterized by a collision centrality, is given in Ref. [38], ranging from 67% centrality for $N_{\text{trk}}^{\text{offline}} = 120$ to 55% centrality for $N_{\text{trk}}^{\text{offline}} = 300$.

4 Analysis

4.1 Scalar product method

In previous publications, CMS has analyzed the elliptic [62] and higher-order [63] flow coefficients for PbPb collisions at $\sqrt{s_{_{\mathrm{NN}}}} = 2.76\,\mathrm{TeV}$ using the "traditional" event plane method [64]. It is now known that fluctuations in the participant geometry lead to v_n coefficients that can vary event-by-event, with the average coefficients $\langle v_n \rangle$ being smaller than the corresponding root-mean-square values, $\sqrt{\langle v_n^2 \rangle}$. The v_n values found using the traditional event plane method will fall somewhere between these two limits [54]. The scalar product method [53, 54], which is used in this paper, avoids this ambiguity and gives results that correspond to $\sqrt{\langle v_n^2 \rangle}$ [54].

The event plane angles can be expressed in terms of Q-vectors. For a perfect detector response, the Q-vector corresponding to the nth-order azimuthal asymmetry for a given event is defined as

$$\begin{aligned} \vec{Q}_n = (Q_{nx}, Q_{ny}) &= \left(\left|\vec{Q}_n\right| \cos(n\Psi_n), \left|\vec{Q}_n\right| \sin(n\Psi_n) \right) \\ &= \left(\sum_{i=1}^{M} w_i \cos(n\phi_i), \sum_{i=1}^{M} w_i \sin(n\phi_i) \right), \end{aligned} \tag{1}$$

where M is the subevent multiplicity, ϕ_i is the azimuthal angle of the ith particle, w_i are weighting factors, and the corresponding event plane angle is given as

$$\Psi_n = \frac{1}{n} \tan^{-1}\left(\frac{Q_{ny}}{Q_{nx}} \right). \tag{2}$$

Different weights w_i are possible. For example, the Q-vectors with $w_i = 1$ relate to the azimuthal particle density, with $w_i = p_{\mathrm{T},i}$ to the transverse momentum distribution, and with $w_i = E_{\mathrm{T},i}$ to the transverse energy distribution. Since the $v_n(p_{\mathrm{T}})$ coefficients increase with p_{T} up to $\approx 3\,\mathrm{GeV}/c$, the choice of either p_{T} or E_{T} weighting generally results in a better event plane angle resolution than a unity particle weighting [64].

Expressed in terms of complex weighted q-vectors, where

$$q_n = \frac{\sum_{i=1}^{M} w_i e^{in\phi_i}}{W}, \tag{3}$$

and $W = \sum_{i=1}^{M} w_i$, the scalar product coefficients are found with

$$v_n\{\mathrm{SP}\} \equiv \frac{\langle q_n q_{n\mathrm{A}}^* \rangle}{\sqrt{\frac{\langle q_{n\mathrm{A}} q_{n\mathrm{B}}^* \rangle \langle q_{nA} q_{n\mathrm{C}}^* \rangle}{\langle q_{n\mathrm{B}} q_{n\mathrm{C}}^* \rangle}}}. \tag{4}$$

In Eq. (4), the weighted average $\langle\rangle$ for vectors $q_{n\alpha}$ and $q_{n\beta}$ with total weights W_α and W_β, where α and β correspond to the second subscripts (if present) on the q-vectors in Eq. (4), is given by

$$\left\langle q_{n\alpha} q_{n\beta}^* \right\rangle = \mathrm{Re}\left[\frac{\sum_{i=1}^{N_{\mathrm{evt}}} W_{\alpha i} W_{\beta i} q_{n\alpha i} q_{n\beta i}^*}{\sum_{i=1}^{N_{\mathrm{evt}}} W_{\alpha i} W_{\beta i}} \right], \tag{5}$$

where N_{evt} is the total number of events. The A, B, and C subscripts in Eq. (4), denoted using α and β in Eq. (5), refer to pseudorapidity ranges for which event planes are determined. Here, the "reference" event plane is the A plane, and the B and C planes are used to correct for the finite resolution of the A plane. The q-vector with only one subscript, q_n in Eq. (4), is based on tracks within the specific p_{T} and η range for which the azimuthal asymmetry coefficient is being measured. Unit weights are used in Eq. (1) in this case.

The two HF calorimeters are used to determine the A and B event planes, with the C plane established using the tracker. In the HF detector regions, with $3.0 < |\eta| < 5.0$, the sums in Eq. (1) are taken over the towers and the weights are taken as the transverse energy deposited in each tower, with no restriction placed on the tower energy. For the tracker-based C plane, the sums are over the individual tracks with $0.3 < p_{\mathrm{T}} < 3.0\,\mathrm{GeV}/c$ and the weights are taken as the corresponding p_{T} values. The Q-vectors corresponding to event planes A, B, and C are "recentered" to account for nonuniformities in the detector response [64, 65]. In recentering, the averages over all events of the x- and y-terms in Eq. (1) ($\langle Q_{nx}\rangle$ and $\langle Q_{ny}\rangle$) are subtracted on an event-by-event basis when calculating $\vec{Q}_n^{\mathrm{Recentered}}$. That is,

$$\vec{Q}_n^{\mathrm{Recentered}} = \left(Q_{nx} - \langle Q_{nx}\rangle\,,\; Q_{ny} - \langle Q_{ny}\rangle\right). \tag{6}$$

The value of q_n in Eq. (4) is based on tracks within a specific p_{T} and η range for which the azimuthal asymmetry coefficient is being measured. In this case, unit weights are used in Eq. (1) and no recentering corrections are applied.

It has been noted recently [66–69], and experimentally confirmed by CMS [70], that the event plane angle should not be considered a global event observable. In the CMS study [70], the decorrelation between the event plane angles at pseudorapidity η_{A} and η_{B} is found to follow the functional form:

$$\cos\left[2\left\{\Psi_n\left(\eta_{\mathrm{B}}\right) - \Psi_n\left(\eta_{\mathrm{A}}\right)\right\}\right] = \mathrm{e}^{-F_n^{\eta}|\eta_{\mathrm{B}}-\eta_{\mathrm{A}}|}, \tag{7}$$

where F_n^{η} is the decorrelation strength.

Such a decorrelation can arise from fluctuations of the geometry of the initial-state nucleons and their constituent partons [66–68]. Previously it has been assumed that Fourier coefficients at pseudorapidity η_{ROI}, where ROI stands for "region of interest", can be deduced using event plane angles found in a different pseudorapidity range (say, at η_{A}), with the caveat that a sufficient pseudorapidity gap is present to avoid short-range correlations. The event plane angle found at η_{A} is viewed as approximating a global participant plane angle set by the initial collision geometry and only differing from the ideal by its finite resolution, which, in turn, depends on both the number of particles used to define the angle and the azimuthal asymmetry at η_{A}. The event plane resolution is accounted for in Eq. (4) by determining event planes in three separate regions of η and assuming that these planes reflect the same underlying geometry, only differing by their respective resolutions. The variation with pseudorapidity breaks this assumption and can have a significant effect on the harmonic coefficient values v_n deduced using either the traditional or scalar product methods.

Considering event plane decorrelation, each of the scalar products in Eq. (4) will be reduced by the decorrelation effect as indicated in Eq. (7). If the decorrelation strength F_n remains relatively constant as a function of the pseudorapidity gap between event planes, the $v_n\{\mathrm{SP}\}$ coefficient in the presence of decorrelation can be expressed in terms of the coefficient without decorrelation

$\bar{v}_n\{\mathrm{SP}\}$ with

$$\begin{aligned} v_n\{\mathrm{SP}\} &= \frac{\langle q_n q_{n\mathrm{A}}^* \rangle \, \mathrm{e}^{-F_n|\eta_\mathrm{A}-\eta_\mathrm{ROI}|}}{\sqrt{\frac{\langle q_{n\mathrm{A}} q_{n\mathrm{B}}^* \rangle \mathrm{e}^{-F_n|\eta_\mathrm{A}-\eta_\mathrm{B}|} \langle q_{n\mathrm{A}} q_{n\mathrm{C}}^* \rangle \mathrm{e}^{-F_n|\eta_\mathrm{A}-\eta_\mathrm{C}|}}{\langle q_{n\mathrm{B}} q_{n\mathrm{C}}^* \rangle \mathrm{e}^{-F_n|\eta_\mathrm{B}-\eta_\mathrm{C}|}}}} \\ &= \bar{v}_n\{\mathrm{SP}\} \frac{\mathrm{e}^{-F_n|\eta_\mathrm{A}-\eta_\mathrm{ROI}|}}{\mathrm{e}^{-\frac{1}{2}F_n\{|\eta_\mathrm{A}-\eta_\mathrm{B}|+|\eta_\mathrm{A}-\eta_\mathrm{C}|-|\eta_\mathrm{C}-\eta_\mathrm{B}|\}}} \\ &= \bar{v}_n\{\mathrm{SP}\} \, \mathrm{e}^{-F_n|\eta_\mathrm{C}-\eta_\mathrm{ROI}|}, \end{aligned} \tag{8}$$

where η_C is taken to fall between η_A and η_B. Short-range, nonflow correlations, such as back-to-back dijets, resonance decay, etc., are again suppressed by having a pseudorapidity gap between η_ROI and η_A.

For the "standard" analysis using a three subevent resolution correction where both the third subevent angle (Ψ_n^C) and the particles belonging to the region of interest are at midrapidity ($\eta_\mathrm{ROI} = \eta_\mathrm{C} \approx 0$), it follows that the decorrelation effect will not strongly influence the deduced Fourier coefficient v_n. It can be noted that the same result is expected if a two-subevent resolution correction is used, as is commonly done for symmetric collision systems. However, if η_ROI is different from η_C, the deduced v_n value will be reduced by the decorrelation effect.

The pseudorapidity-dependent decorrelation of event planes can occur through different mechanisms. Equation (8) assumes a Gaussian decorrelation characterized by a fixed F_n value. It is also possible for F_n^η to vary with η, in which case the η dependence shown in Eq. (7) and (8) would be more complicated. A simplified MC simulation was used to explore the two Gaussian spreading scenarios, corresponding to a fixed or η-dependent F_n^η factor. It was found that the input v_n values could be recovered by moving the Ψ_n^C event plane along with the particles of interest. An alternative source of decorrelation is the situation where rotation of the event plane angle results from a torque effect rather than a random spreading [67]. In this case, the MC simulations showed that moving the Ψ_n^C event plane does not fully correct for the decorrelation, although it does lead to results closer to the input values than is found by setting $\eta_\mathrm{C} = 0$. A comparison of the v_2 and v_3 results obtained with $\eta_\mathrm{C} = 0$ and with $\eta_\mathrm{C} = \eta_\mathrm{ROI}$ might help in estimating the relative importance of the different types of decorrelation possible in heavy ion collisions. Event plane results using both of these assumptions for η_C are reported.

Two different reference event planes are used in the analysis: HF^- $(-5.0 < \eta < -3.0)$ and HF^+ $(3.0 < \eta < 5.0)$. The corresponding resolution correction factors are determined with the three subevent method where, for the $\mathrm{HF}^+(\mathrm{HF}^-)$ reference plane (A-plane), the resolution correction is based on the $\mathrm{HF}^-(\mathrm{HF}^+)$ event plane (B-plane) as well as either the midrapidity tracker event plane, with $-0.8 < \eta < 0.8$, or with event planes that correspond to the pseudorapidity range of the ROI (C-plane). Since analyses where the midrapidity event plane η_C is taken within $-0.8 < \eta_\mathrm{C} < 0.8$ and analyses where $\eta_\mathrm{C} = \eta_\mathrm{ROI}$ are both presented, the convention is adopted of labelling results as "$\eta_\mathrm{C} = 0$" or "$\eta_\mathrm{C} = \eta_\mathrm{ROI}$," respectively.

4.2 Cumulant method

If the particles emitted in a collision are correlated with a global reference frame, they will also be correlated with each other. The cumulant method explores the collective nature of the anisotropic flow through the multiparticle correlations. As the number of particles in the correlation study increases, the cumulant values will decrease if only part of the particle sample shares a common underlying symmetry, as would be the case for dijets. The flow harmonics are studied using the Q-cumulant method [51]. The m-particle ($m = 2$, 4, 6 or 8) nth-order correlators are first defined by

$$\begin{aligned}
\langle\langle 2\rangle\rangle &\equiv \left\langle\left\langle e^{in(\phi_1-\phi_2)}\right\rangle\right\rangle,\\
\langle\langle 4\rangle\rangle &\equiv \left\langle\left\langle e^{in(\phi_1+\phi_2-\phi_3-\phi_4)}\right\rangle\right\rangle,\\
\langle\langle 6\rangle\rangle &\equiv \left\langle\left\langle e^{in(\phi_1+\phi_2+\phi_3-\phi_4-\phi_5-\phi_6)}\right\rangle\right\rangle,\\
\langle\langle 8\rangle\rangle &\equiv \left\langle\left\langle e^{in(\phi_1+\phi_2+\phi_3+\phi_4-\phi_5-\phi_6-\phi_7-\phi_8)}\right\rangle\right\rangle,
\end{aligned} \tag{9}$$

where ϕ_i is the azimuthal angle of the ith particle, and $\langle\langle\ldots\rangle\rangle$ indicates that the average is taken over all m-particle combinations for all events. In order to remove self-correlations, it is required that the m particles be distinct. The unbiased estimators of the reference m-particle cumulants [51], $c_n\{m\}$, are defined as

$$\begin{aligned}
c_n\{4\} =&\langle\langle 4\rangle\rangle - 2\,\langle\langle 2\rangle\rangle^2,\\
c_n\{6\} =&\langle\langle 6\rangle\rangle - 9\,\langle\langle 4\rangle\rangle\langle\langle 2\rangle\rangle + 12\,\langle\langle 2\rangle\rangle^3,\\
c_n\{8\} =&\langle\langle 8\rangle\rangle - 16\,\langle\langle 6\rangle\rangle\langle\langle 2\rangle\rangle - 18\,\langle\langle 4\rangle\rangle^2\\
&+ 144\,\langle\langle 4\rangle\rangle\langle\langle 2\rangle\rangle^2 - 144\,\langle\langle 2\rangle\rangle^4.
\end{aligned} \tag{10}$$

The reference flow $v_2\{m\}$ obtained by correlating the m particles within the reference phase space of $|\eta| < 2.4$ and p_T range of $0.3 < p_T < 3.0\,\mathrm{GeV}/c$ was presented in Ref. [39] using

$$\begin{aligned}
v_n\{4\} &= \sqrt[4]{-c_n\{4\}}\\
v_n\{6\} &= \sqrt[6]{c_n\{6\}/4},\\
v_n\{8\} &= \sqrt[8]{-c_n\{8\}/33}.
\end{aligned} \tag{11}$$

The cumulant calculations are done using the code described in Ref. [71].

By replacing one of the particles in a correlator for each term in Eq. (9) with a particle from certain ROI phase space in p_T or η, with the corresponding correlators denoted by primes, one can derive the differential m-particle cumulants as

$$\begin{aligned}
d_n\{4\} =&\langle\langle 4'\rangle\rangle - 2\langle\langle 2\rangle\rangle\langle\langle 2'\rangle\rangle,\\
d_n\{6\} =&\langle\langle 6'\rangle\rangle - 6\langle\langle 2\rangle\rangle\langle\langle 4'\rangle\rangle - 3\langle\langle 2'\rangle\rangle\langle\langle 4\rangle\rangle + 12\langle\langle 2'\rangle\rangle\langle\langle 2\rangle\rangle^2,\\
d_n\{8\} =&\langle\langle 8'\rangle\rangle - 12\langle\langle 2\rangle\rangle\langle\langle 6'\rangle\rangle - 4\langle\langle 2'\rangle\rangle\langle\langle 6\rangle\rangle\\
&- 18\langle\langle 4'\rangle\rangle\langle\langle 4\rangle\rangle + 72\langle\langle 4\rangle\rangle\langle\langle 2\rangle\rangle\langle\langle 2'\rangle\rangle\\
&+ 72\langle\langle 4'\rangle\rangle\langle\langle 2\rangle\rangle^2 - 144\langle\langle 2'\rangle\rangle\langle\langle 2\rangle\rangle^3.
\end{aligned} \tag{12}$$

Then the differential $v_2\{m\}(p_T,\eta)$ can be extracted as

$$\begin{aligned}
v_n\{4\}(p_T,\eta) &= -d_n\{4\}/(-c_n\{4\})^{3/4},\\
v_n\{6\}(p_T,\eta) &= \frac{d_n\{6\}}{4}\Big/\left(\frac{c_n\{6\}}{4}\right)^{5/6},\\
v_n\{8\}(p_T,\eta) &= \frac{-d_n\{8\}}{33}\Big/\left(\frac{-c_n\{8\}}{33}\right)^{7/8}.
\end{aligned} \tag{13}$$

An efficiency weight is applied to each track to account for detector nonuniformity and efficiency effects. For this analysis, the work of Ref. [71] was extended to allow for the explicit calculation of the differential Q-cumulants for the first time.

4.3 Lee–Yang zeros method

The LYZ method [52] allows for a direct study of the large-order behavior by using the asymptotic form of the cumulant expansion to relate locations of the zeros of a generating function to the azimuthal correlations. This method has been employed in previous CMS PbPb and pPb analyses [39, 62, 63]. The v_2 harmonic averaged over $0.3 < p_T < 3.0\,\text{GeV}/c$ is found for each multiplicity bin using an integral generating function [17]. Similar to the cumulant methods, a weight for each track is implemented to account for detector-related effects. Anisotropic flow is formally equivalent to a first-order phase transition. As a result, the first zero of the generating grand partition function can be viewed as anisotropic flow of the final-state system.

The integrated flow for the harmonic n is the average value of the flow Q-vector projected onto the unit vector with angle $n\Phi_R$,

$$v_n^{\text{int}} \equiv \left\langle Q_{nx} \cos\left(n\Phi_R\right) + Q_{ny} \sin\left(n\Phi_R\right)\right\rangle = \left\langle Q_n^{\Phi_R} \right\rangle, \tag{14}$$

where Φ_R is the actual reaction-plane angle. Since Φ_R is not an observable, the LYZ method is used to obtain an estimate of this quantity. In the present analysis, a complex product generating function is first defined as

$$G_n^\theta(ir) = \left\langle g_n^\theta(ir) \right\rangle = \left\langle \prod_{j=1}^{M} [1 + ir\, w_j \cos\left(n(\phi_j - \theta)\right)] \right\rangle, \tag{15}$$

where M is the event multiplicity, ϕ_j and w_j are, respectively, the azimuthal angle and the weight of the jth particle, the average $\langle\rangle$ is taken over all events, and θ is chosen to take discrete values within the range $[0, \pi/n)$ as

$$\theta = \frac{k}{n_\theta}\frac{\pi}{n}, \quad k = 0, 1, 2, ..., n_\theta - 1. \tag{16}$$

The number of projection angles is set to $n_\theta = 5$ to get the average values. This number was found in the previous CMS studies to achieve convergence of the results [39, 62, 63].

To calculate the yield-weighted integral flow, G_n^θ is evaluated for many values of the real positive variable r. Plotting the modulus $|G_n^\theta(ir)|$ as a function of r, the integrated flow is directly related to the first minimum r_0^θ of the distribution, with

$$v_n^{\theta,\text{int}}\{\infty\} \equiv \frac{j_{01}}{r_0^\theta}, \tag{17}$$

where $j_{01} \approx 2.405$ is the first root of the Bessel function $J_0(x)$. The quoted results involve a final average over different θ values, with

$$v_n^{\text{int}} = \frac{1}{n_\theta} \sum_{\theta=0}^{n_\theta - 1} v_n^{\theta,\text{int}}\{\infty\}. \tag{18}$$

After the integrated flow coefficient v_n^{int} is determined, the p_T- and η-dependent $v_2\{\text{LYZ}\}$ values are found using

$$\frac{v_n^\theta}{v_n^{\theta,\text{int}}} = \text{Re}\, \frac{\left\langle g^\theta(ir_0^\theta) \frac{cos(n(\phi_j - \theta))}{1 + ir_0^\theta w_j \cos\left(n(\phi_j - \theta)\right)} \right\rangle_\phi}{\left\langle g^\theta(ir_0^\theta) \sum_j \frac{w_j cos(n(\phi_j - \theta))}{1 + ir_0^\theta w_j \cos\left(n(\phi_j - \theta)\right)} \right\rangle}. \tag{19}$$

The average $\langle ... \rangle_\phi$ in the numerator is taken over the particles in the ROI. The average in the denominator is over all particles with $0.3 < p_T < 3.0\,\text{GeV}/c$ and $|\eta| < 2.4$. Again, the final results involve an average over the different θ values

$$v_n = \frac{1}{n_\theta} \sum_{\theta=0}^{n_\theta - 1} v_n^\theta. \tag{20}$$

4.4 Systematic uncertainties

The systematic uncertainties resulting from the track selection and efficiency, from the vertex position, and from the pileup contamination contribute to all three methods (scalar product, cumulant, and LYZ). The effects of track quality requirements were studied by varying the track selection requirements, $d_z/\sigma(d_z)$ and $d_T/\sigma(d_T)$, from 2 to 5, and $\sigma(p_T)/p_T$ from 5% to the case where this requirement is not applied. A comparison of the results using efficiency correction tables from EPOS and HIJING MC event generators was made to study the tracking efficiency uncertainty. By comparing the results from different event primary vertex positions along the beam direction, with $|z_{vtx}| < 3\,\text{cm}$ and $3 < |z_{vtx}| < 15\,\text{cm}$, it is possible to investigate the uncertainties coming from the tracking acceptance effects. The effects of pileup events were studied by looking at events where there was only one reconstructed vertex. The experimental systematic effects are found to have no significant dependence on $N_{trk}^{offline}$, p_T, or η.

The v_2 systematic uncertainties associated with the PbPb collision results were found to be comparable for the three methods ($\approx$3%), with contributions from the track selection and efficiency (1–2%), the vertex position (1–2%), and pileup effects (<1%). Similar uncertainties are found for pPb collisions based on both the cumulant and scalar product methods. For the LYZ pPb results, a more conservative uncertainty of 11% is quoted based on the large statistical uncertainties associated with the corresponding systematic studies.

In addition, a comparison was done between the results for the two different beam directions. For the event plane analysis, the p-side and Pb-side HF detectors used to determine the event plane angles are switched by changing the beam direction. Based on this study, where the small magnitude of the v_3 coefficient limits the statistical significance of the systematic studies, a larger, conservative systematic uncertainty is assigned to the $v_3\{\text{SP}\}$ results of 10%. The overall systematic uncertainties are summarized in Table 1, and shown as grey boxes in the figures.

Table 1: Systematic uncertainties.

		$v_2(p_T)$	$v_2(\eta)$	v_3
Scalar product	pPb	3%	3%	10%
	PbPb	3%	3%	10%
Cumulant	pPb	3%	3%	—
	PbPb	3%	3%	—
Lee–Yang zeros	pPb	11%	11%	—
	PbPb	3%	3%	—

The multiparticle cumulant and LYZ analyses are expected to be relatively insensitive to nonflow effects. For the scalar product method, however, the nonflow effects can become significant as the differential particle density decreases, as is the situation for the lower $N_{trk}^{offline}$ ranges and for higher p_T values. Also, the nonflow effects become more significant as the gap between the primary event plane (η_A) and the region of interest (η_{ROI}) becomes small. In this paper, the nonflow influence on the scalar product results is viewed as part of the physics being explored and is not taken as a systematic uncertainty.

5 Results

We first explore the transverse momentum dependence of v_2 and v_3 in pPb and PbPb at comparable particle multiplicities. The v_2 values were found using the scalar product, m-particle cumulant, and LYZ methods, denoted as $v_2\{SP\}$, $v_2\{m\}$, and $v_2\{LYZ\}$, respectively, while v_3 was found using only the scalar product method.

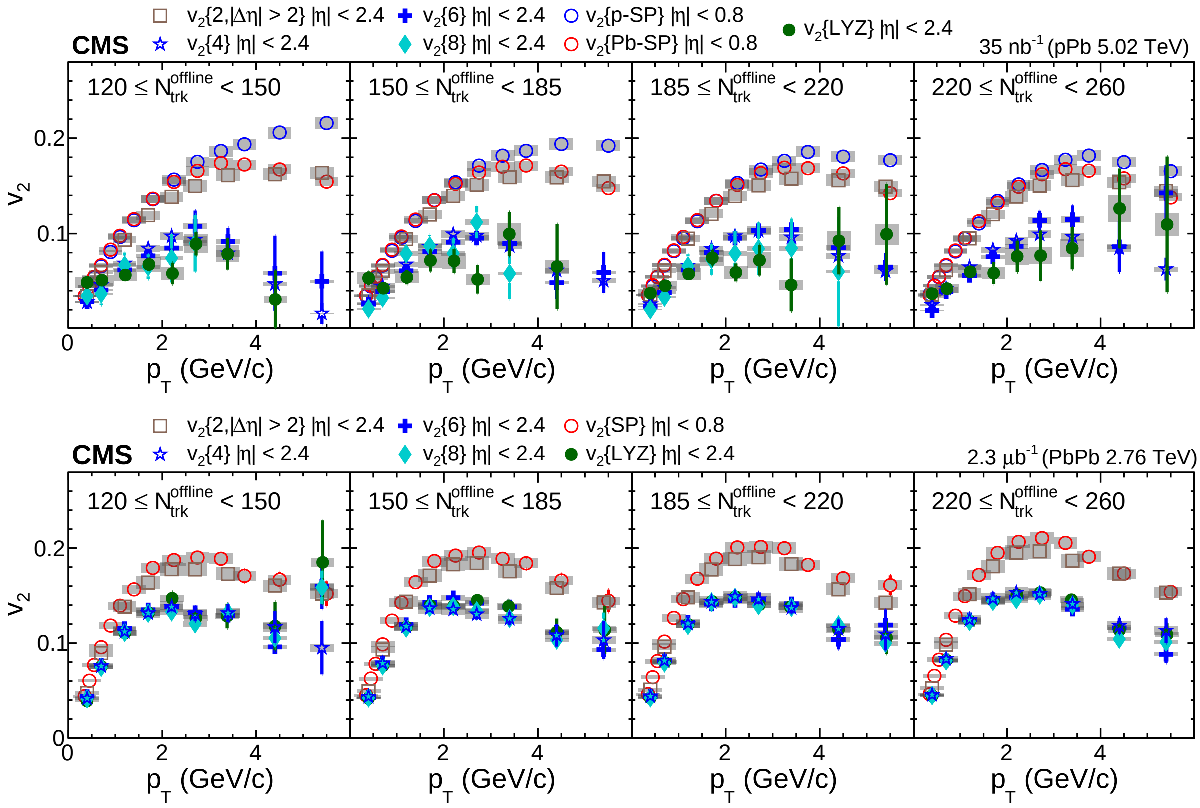

Figure 1: (Color online) (Top) The v_2 coefficients as a function of p_T in pPb collisions for different $N_{trk}^{offline}$ ranges. (Bottom) Same, but for PbPb collisions. The $v_2\{2, |\Delta\eta| > 2\}$ and $v_2\{4\}$ results are from Ref. [38]. For the pPb collisions, the notations p-SP and Pb-SP indicate the pseudorapidity side of the reference event plane, and correspond to the p- and Pb-going directions, respectively. Pseudorapidities are given in the laboratory frame. Systematic uncertainties are indicated by the grey boxes.

The momentum-dependent $v_2(p_T)$ results in the region $|\eta| < 2.4$ for pPb and PbPb collisions are shown in Fig. 1. The scalar product values, shown separately for the p- and Pb-going event planes, are found to be significantly higher than the multiparticle cumulant ($v_2\{4\}$, $v_2\{6\}$, and $v_2\{8\}$), and Lee–Yang zeros ($v_2\{LYZ\}$) results. The two-particle correlations ($v_2\{2\}$) and lower-order cumulant ($v_2\{4\}$) measurements shown in the figure are from Ref. [38]. As will be discussed when presenting the yield-weighted integral v_2 values, the greater values found for $v_2\{SP\}$ and $v_2\{2\}$ suggest a significant, and expected, contribution of fluctuations in the initial-state geometry to these results.

In the range of $p_T < 2\,\text{GeV}/c$ there is very little difference between the $v_2\{\text{SP}\}$ results obtained with the p- and Pb-going side event planes. However, at higher transverse momenta, the p-going event plane leads to systematically larger values. This behavior suggests that the nonflow contribution has a larger effect on the high-p_T v_2 values based on the p-going side event plane. Monte Carlo simulations using the HIJING event generator support a nonflow component to the v_2 signal that increases almost monotonically with p_T. In situations where both the event plane angle and the Q-vector associated with the region of interest are based on small numbers of particles, the nonflow behavior can be significant. It is also possible that the p_T-dependent event-plane decorrelation effects might be different on the Pb- and p-going sides.

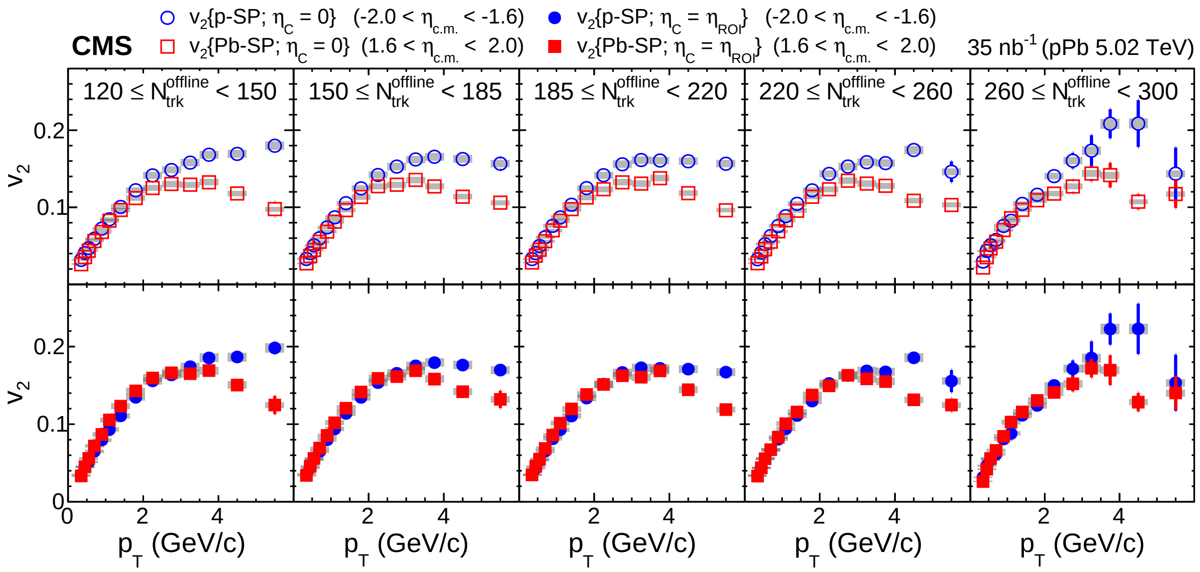

Figure 2: (Color online) (Top) Comparison of $v_2(p_T)$ distributions located on the Pb-going ($-2.0 < \eta_{\text{c.m.}} < -1.6$) and p-going ($1.6 < \eta_{\text{c.m.}} < 2.0$) sides of the tracker region, with $\eta_C = 0$. The notations p-SP and Pb-SP indicate the pseudorapidity side of the reference event plane and correspond to the p- and Pb-going directions, respectively. (Bottom) Same, but with $\eta_C = \eta_{\text{ROI}}$, as discussed in the text. Pseudorapidities are given in the laboratory frame. Systematic uncertainties are indicated by the grey boxes.

In contrast to Fig. 1, which uses an η region that is symmetric in the lab frame, Fig. 2 compares the $v_2\{\text{SP}\}(p_T)$ results for symmetric pseudorapidity ranges in the center-of-mass frame. The laboratory frame results for the range of $2.0 < \eta < 2.4$ correspond approximately to the center-of-mass range of $1.6 < \eta_{\text{c.m.}} < 2.0$ and are obtained with respect to the event plane found on the Pb-going side with $-5.0 < \eta < -3.0$, as indicated with the notation v_2 {Pb-SP}. Similarly, the range of $-1.6 < \eta < -1.2$ approximately corresponds to $-2.0 < \eta_{\text{c.m.}} < -1.6$. Here the results are obtained with respect to the event plane found on the p-going side with $3.0 < \eta < 5.0$, as indicated with the notation v_2 {p-SP}. The measured values are shown separately with $\eta_C = 0$ and $= \eta_{\text{ROI}}$. The reference event plane used in each case corresponds to the more distant HF detector. In the region with $1.5 < p_T < 3.0\,\text{GeV}/c$, the enhancement observed on the Pb-going side ($-2.0 < \eta_{\text{c.m.}} < -1.6$; p-SP) with $\eta_C = 0$ (top row) is reduced by taking $\eta_C = \eta_{\text{ROI}}$ (bottom row). This dependence on η_C suggests the presence of event plane decorrelation.

Further evidence for event plane decorrelation is seen by comparing the pseudorapidity dependence of the yield-weighted v_2 values for $0.3 < p_T < 3.0\,\text{GeV}/c$. This is shown in Figs. 3 and 4 for the pPb and PbPb collisions, respectively. The top row in each figure shows the scalar product results with $\eta_C = 0$ and the bottom row with $\eta_C = \eta_{\text{ROI}}$. For the pPb collisions, results

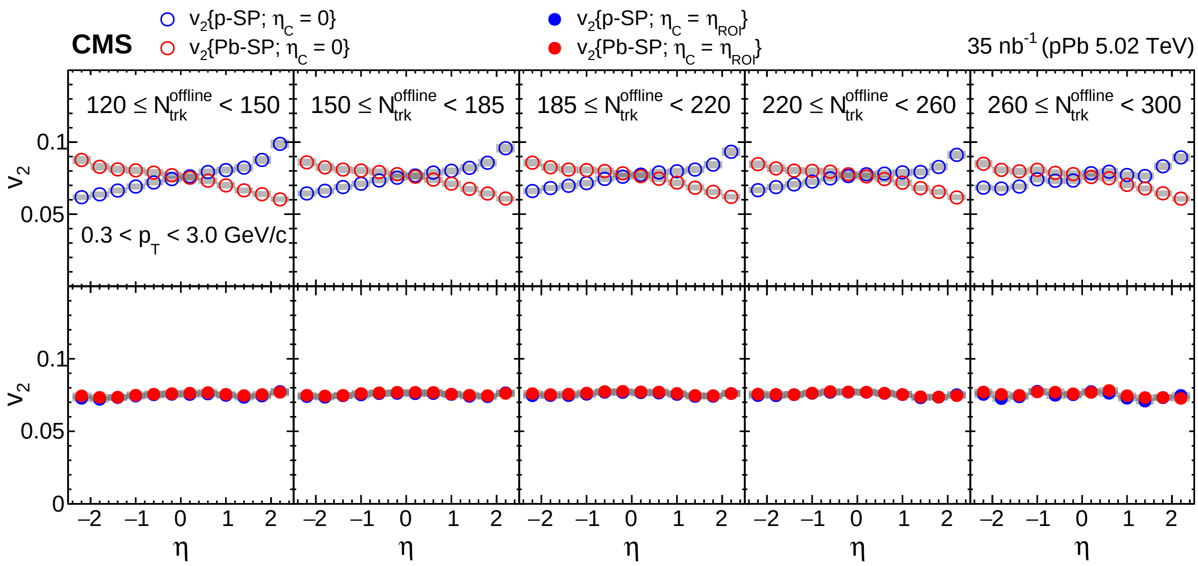

Figure 3: (Color online) (Top) Yield-weighted $v_2\{\mathrm{SP}\}$ with $0.3 < p_{\mathrm{T}} < 3.0\,\mathrm{GeV}/c$ as a function of η in pPb collisions for different $N_{\mathrm{trk}}^{\mathrm{offline}}$ ranges with $\eta_{\mathrm{C}} = 0$. (Bottom) Same, but with $\eta_{\mathrm{C}} = \eta_{\mathrm{ROI}}$. The notations p-SP and Pb-SP indicate the pseudorapidity side of the reference event plane and correspond to the p- and Pb-going directions, respectively. Pseudorapidities are given in the laboratory frame. Systematic uncertainties are indicated by the grey boxes.

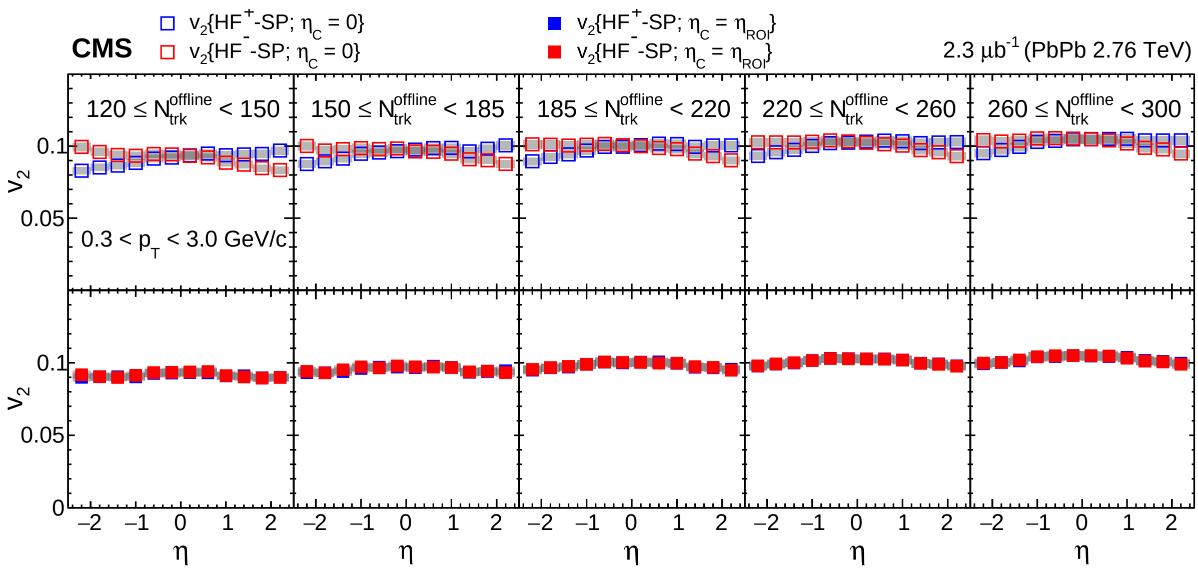

Figure 4: (Color online) (Top) Yield-weighted $v_2\{\mathrm{SP}\}$ coefficients as a function of η in PbPb collisions for different $N_{\mathrm{trk}}^{\mathrm{offline}}$ ranges with $\eta_{\mathrm{C}} = 0$. (Bottom) Same, but with $\eta_{\mathrm{C}} = \eta_{\mathrm{ROI}}$. The notations HF^{+} and HF^{-} indicate the pseudorapidity side of the reference event plane. Pseudorapidities are given in the laboratory frame. Systematic uncertainties are indicated by the grey boxes.

are shown separately over the full pseudorapidity range of the CMS tracker using the HF event planes on the p- and Pb-going side of the collision. For the symmetric PbPb collisions, the results using the HF^+ and HF^- event planes are shown separately. The yield-weighted elliptic flow coefficients for PbPb collision are found to be ≈20% larger than for pPb collisions. In the absence of decorrelation effects, the choice of $\eta_C = 0$ or $= \eta_{ROI}$ would be expected to result in similar distributions. In previous PbPb studies [62, 63], taking $\eta_C = 0$, the $v_2(\eta)$ values with $\eta < 0$ were reported using the event plane with $3.0 < \eta < 5.0$, and the values with $\eta > 0$ were reported using the event plane with $-5.0 < \eta < -3.0$, thus achieving the largest possible gap in pseudorapidity. Before accounting for an increasing decorrelation of event planes with an increasing pseudorapidity gap, the v_2 values based on p-going and Pb-going side event planes (pPb collisions) or HF^+ and HF^- event planes (PbPb collisions) show different pseudorapidity dependences, with the values decreasing as the gap with the reference event plane increases. This reference event plane dependence largely disappears once a correction is applied for decorrelation effects, with the corrected v_2 values showing very little pseudorapidity dependence. The resulting boost invariance is consistent with the azimuthal dependence being determined by the initial-state geometry. For the pPb collisions, the results with $2.0 < \eta < 2.4$ determined using the p-going side reference event plane are systematically higher in each of the $N_{trk}^{offline}$ ranges. This is consistent with the reduced multiplicity associated with this eta region, allowing for an increased influence of nonflow effects.

The current results suggest that event plane decorrelation effects might be significant in trying to understand the pseudorapidity dependence of the flow coefficients. The results with $2.0 < \eta < 2.4$ determined using the p-going side reference event plane are systematically higher, suggesting the possible influence of nonflow effects.

Expanding on the results in Figs. 3 and 4, which show only v_2 from the scalar product method, the yield-weighted average v_2 values for all of the analysis methods are shown in Fig. 5. It is interesting to note that the pseudorapidity dependence is almost flat for the scalar product calculations where $\eta_C = \eta_{ROI}$. This is in contrast to the scalar product results for $\eta_C = 0$ and for the higher-order particle correlation analyses, where the v_2 values at larger pseudorapidities are significantly smaller. It is only for the scalar product analysis with $\eta_C = \eta_{ROI}$ that a partial accounting for the event plane decorrelation behavior is achieved. Both the cumulant and LYZ analyses employ integral reference flows based on the full range of the CMS tracker and thus are not able to account for decorrelation effects. There is an apparent asymmetry as a function of pseudorapidity for the LYZ results for the two highest $N_{trk}^{offline}$ ranges, with a larger v_2 signal observed on the Pb-going side event plane. Although this asymmetry appears to be larger than that found for the cumulant or scalar product analyses, the large statistical uncertainties make a direct comparison difficult.

It can be seen from Fig. 5 that the PbPb results for a given $N_{trk}^{offline}$ range are consistently higher than the corresponding pPb results. This likely reflects the very different collision geometries for the two systems, with the elliptic flow for PbPb collisions being influenced by the lenticular-shaped overlap region developed in non-central collisions of two Pb nuclei. In a later discussion, this result will be contrasted with a similar comparison for the v_3 harmonic.

As already suggested for the p_T-dependent results, the difference between the scalar product and two-particle correlations results, as compared to the higher-order correlation studies, is likely to reflect initial-state fluctuation effects. Event-by-event fluctuations in the location of the participant nucleons can have a large and method-dependent influence on the harmonic coefficients [72, 73]. Expressing the fluctuations in terms of the azimuthal anisotropy in the participant plane v, where the harmonic number is suppressed, the magnitude of the fluctuations

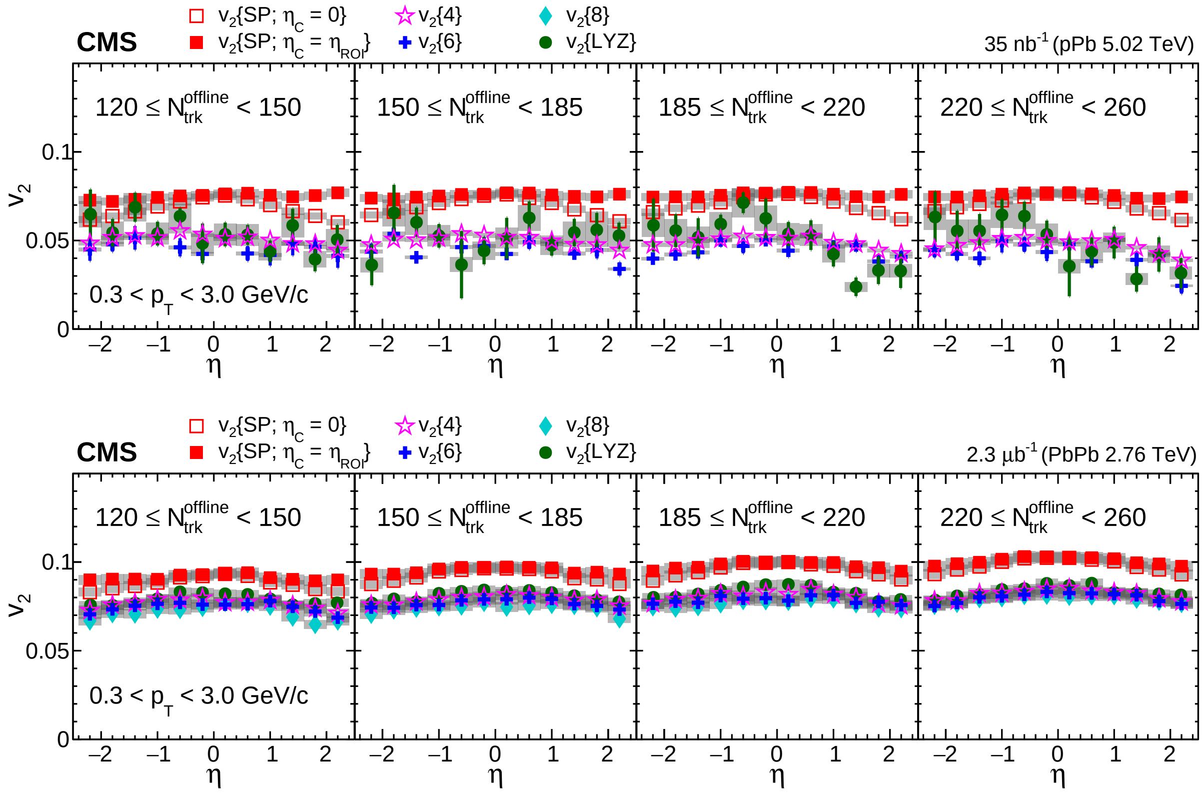

Figure 5: (Color online) (Top) Yield-weighted v_2 values calculated using the scalar product, cumulant, and LYZ methods as a function of η in pPb collisions for different $N_{\mathrm{trk}}^{\mathrm{offline}}$ ranges. (Bottom) Same, but for PbPb collisions. The $v_2\{\mathrm{SP}\}$ results are based on the furthest HF event plane in pseudorapidity from the particles of interest. Pseudorapidities are given in the laboratory frame. Systematic uncertainties are indicated by the grey boxes.

is given by $\sigma_v^2 \equiv \langle v^2 \rangle - \langle v \rangle^2$. To leading order in σ_v [73], two- and four-particle correlations are affected differently, with

$$v\{2\}^2 = \langle v^2 \rangle = \langle v \rangle^2 + \sigma_v^2 \tag{21}$$

and

$$v\{4\}^2 = \left(2\langle v^2 \rangle^2 - \left\langle v^4 \right\rangle\right)^{1/2} \approx \langle v \rangle^2 - \sigma_v^2. \tag{22}$$

Multiparticle correlations with more than four particles are expected to give results similar to those of four-particle correlations. Fluctuations affect the scalar product and two-particle correlations in a similar manner. The difference between the scalar product and higher-order cumulant results therefore reflects the initial-state fluctuations.

Using Eqs. (21) and (22), the fluctuation ratio $\sigma_v / \langle v \rangle$ can be calculated as

$$\frac{\sigma_v}{\langle v \rangle} = \sqrt{\frac{v_2\{2\}^2 - v_2\{4\}^2}{v_2\{2\}^2 + v_2\{4\}^2}} = \sqrt{\frac{v_2\{\mathrm{SP}\}^2 - v_2\{4\}^2}{v_2\{\mathrm{SP}\}^2 + v_2\{4\}^2}}. \tag{23}$$

This ratio is shown in Fig. 6 for the pPb and PbPb collisions in different $N_{\mathrm{trk}}^{\mathrm{offline}}$ ranges. The $v_2\{\mathrm{SP}\}$ results with $\eta_C = 0$ are used in the calculations since the $v_2\{4\}$ results are expected to be affected by decorrelation effects. The fluctuation component is found to be significantly larger for the pPb collisions as compared to the PbPb results. A small (15–20%) increase in the ratio is found for both the pPb and PbPb systems as the $N_{\mathrm{trk}}^{\mathrm{offline}}$ range increases. The pPb system also shows an increase in the ratio as the pseudorapidity increases.

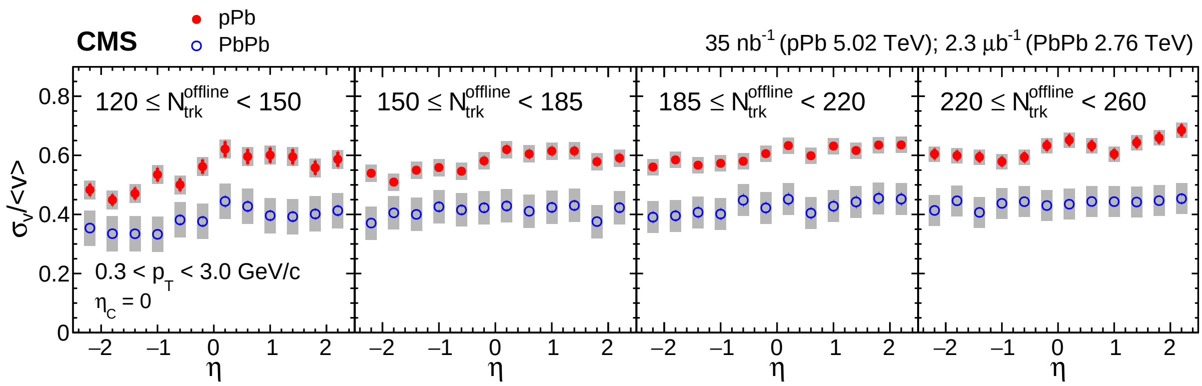

Figure 6: (Color online) The ratio $\sigma_v / \langle v \rangle$ in the pPb and PbPb systems as a function of pseudorapidity for the indicated $N_{\mathrm{trk}}^{\mathrm{offline}}$ ranges. Pseudorapidities are given in the laboratory frame. Systematic uncertainties are indicated by the grey boxes.

The results presented here can be used to evaluate in more detail previous CMS analyses which suggest a significant pseudorapidity dependence of the v_2 coefficient of pPb collisions, with a larger "flow" signal on the Pb-going side [74]. That study was based on a two-particle correlation analysis and focused on the ratio $v_2(\eta)/v_2(\eta = 0)$. Since the Ref. [74] analysis does not take into account decorrelation effects, it is most closely related to the scalar product analysis with $\eta_C = 0$ and to the multiparticle correlation measurements based on the integral flow coefficients found using an extended range of the CMS tracker acceptance. The Ref. [74] results are compared to the scalar product and four-particle cumulant results in Fig. 7. Agreement is found among these measurements. The scalar product results with $\eta_C = \eta_{\mathrm{ROI}}$, also shown in Fig. 7, fall off more slowly when moving away from midrapidity.

To explore further the possible asymmetry in the pseudorapidity-dependent v_2 results of Fig. 5 for the pPb system, Fig. 8 shows the ratios of the yield-weighted integral values on the p- and

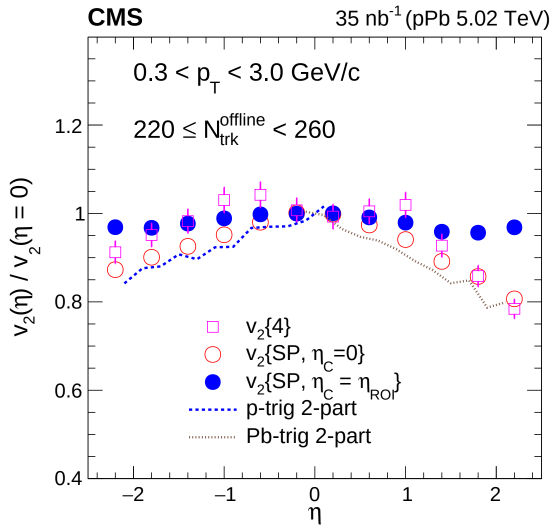

Figure 7: (Color online) Comparison of the scalar product ($v_2\{\mathrm{SP}\}$) and cumulant ($v_2\{4\}$) results for the ratio $v_2(\eta)/v_2(\eta = 0)$ with the two-particle correlation results from Ref. [74] for pPb collisions at $\sqrt{s_{_{\mathrm{NN}}}} = 5.02\,\mathrm{TeV}$ and with $220 \le N_{\mathrm{trk}}^{\mathrm{offline}} < 260$. The scalar product results with $\eta < 0$ use the p-side reference event plane with $3.0 < \eta < 5.0$, and the results with $\eta > 0$ are based on the Pb-side reference event plane with $-5.0 < \eta < -3.0$. The two-particle correlation results of Ref. [74] for p-side (p-trig 2-part) and Pb-side (Pb-trig 2-part) trigger particles are shown without the peripheral v_2 component subtraction, a correction for nonflow effects that increases the v_2 harmonics. Pseudorapidities are given in the laboratory frame. Error bars are statistical uncertainties.

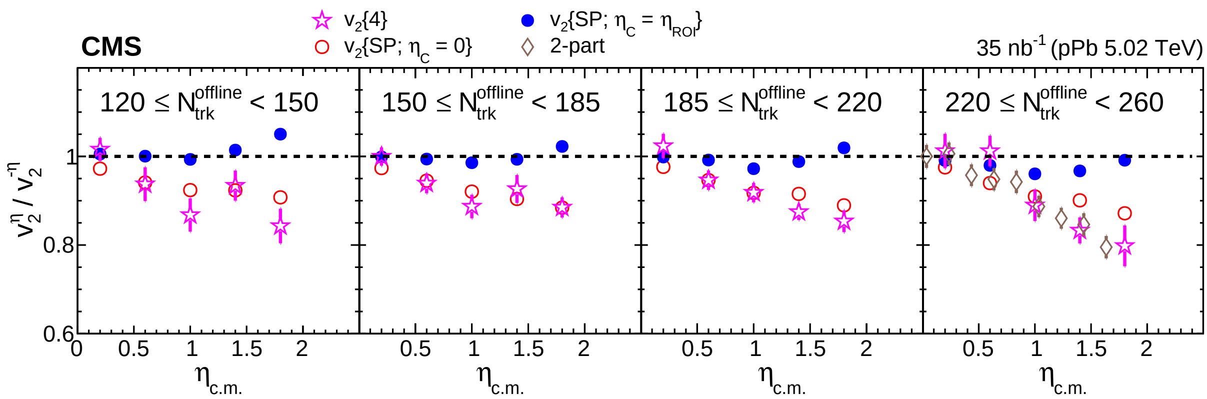

Figure 8: (Color online) Ratio of the p- to Pb-going side v_2 coefficients at comparable $\eta_{\mathrm{c.m.}}$ values for pPb collisions. The two-particle correlation results (labelled “2-part”) are from Ref. [74]. The reference *HF* event plane is the one furthest from the particles of interest.

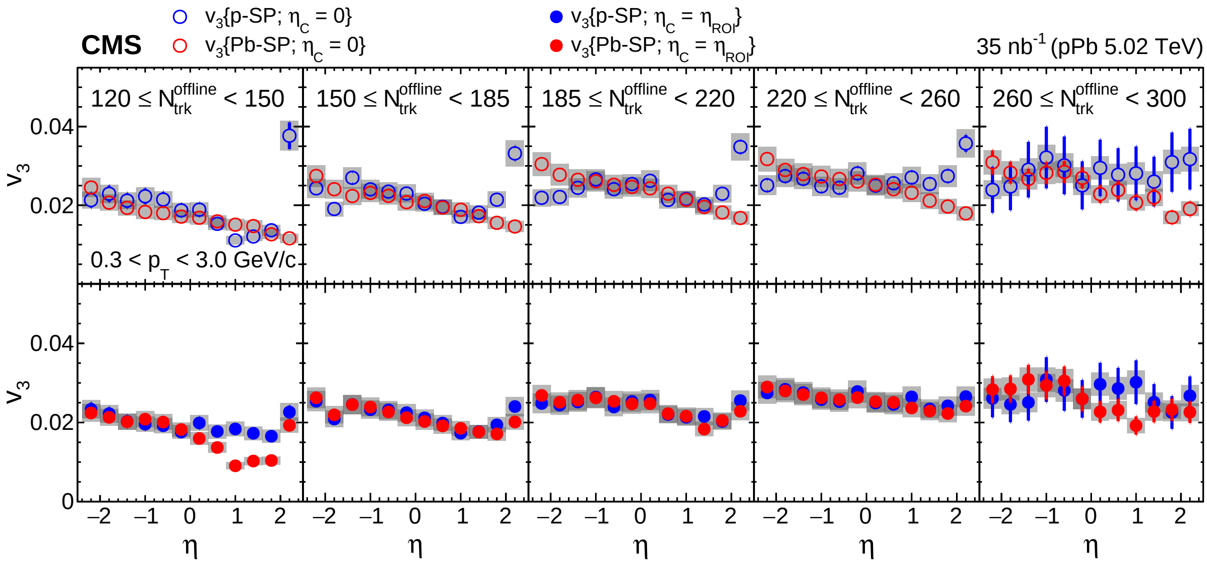

Figure 9: (Color online) (Top) The v_3 values from the scalar product method for pPb collisions at $\sqrt{s_{\mathrm{NN}}} = 5.02\,\mathrm{TeV}$ with $\eta_{\mathrm{C}} = 0$. (Bottom) Same, but with $\eta_{\mathrm{C}} = \eta_{\mathrm{ROI}}$. The notations p-SP and Pb-SP indicate the pseudorapidity side of the reference event plane and correspond to the p- and Pb-going directions, respectively. Pseudorapidities are given in the laboratory frame. Systematic uncertainties are indicated by the grey boxes.

Pb-going sides at comparable center-of-mass pseudorapidity for pPb collisions. The results are shown for the scalar product analyses with $\eta_{\mathrm{C}} = 0$ and $= \eta_{\mathrm{ROI}}$, and for the four-particle cumulant analysis. Also shown are the comparable results from the Ref. [74] analysis. For the pPb results where decorrelation effects are not taken into account (i.e., $v_2\{\mathrm{SP}, \eta_{\mathrm{C}} = 0\}$ and $v_2\{4\}$), the Pb-going side values are significantly larger. The asymmetry between the Pb-going and p-going sides largely disappears when decorrelation effects are taken into account. A small asymmetry continues to be present when decorrelation effects are considered (i.e., $v_2\{\mathrm{SP}, \eta_{\mathrm{C}} = \eta_{\mathrm{ROI}}\}$), although it needs to be recognized that the procedure of moving the η_{C} range with η_{ROI} is not expected to fully account for these effects if a torque-effect decorrelation is present; there may be some additional influence of nonflow effects when the η gap between the η_{C} and either the η_{A} or η_{B} event planes becomes small.

In contrast to the second order Fourier coefficients discussed above, triangular flow, corresponding to the v_3 Fourier harmonic, is believed to arise from fluctuations in the participant geometry in collisions of heavy nuclei. It is interesting to see how this behavior extends to the very asymmetric pPb system. Fig. 9 shows the scalar product results for the pPb collisions at $\sqrt{s_{\mathrm{NN}}} = 5.02\,\mathrm{TeV}$ with $\eta_{\mathrm{C}} = 0$ (top) and $= \eta_{\mathrm{ROI}}$ (bottom), respectively, as a function of η. Yield-weighted v_3 values with $0.3 < p_{\mathrm{T}} < 3.0\,\mathrm{GeV}/c$ are shown. A pronounced jump in v_3, which becomes smaller with increasing $N_{\mathrm{trk}}^{\mathrm{offline}}$, is observed for $\eta > 2$ when using the p-going side reference event plane. This could be due to nonflow effects when the ROI is close to the reference event plane. For the Pb-going side reference event plane, a similar, but much smaller effect, may be present when taking $\eta_{\mathrm{C}} = \eta_{\mathrm{ROI}}$.

A small pseudorapidity dependence is seen in the $v_3\{\eta_{\mathrm{C}} = \eta_{\mathrm{ROI}}\}$ results, with the values becoming smaller on the p-going side. This might suggest a changing level of fluctuations driving the triangular flow signal. The pseudorapidity dependence appears to become less significant as $N_{\mathrm{trk}}^{\mathrm{offline}}$ increases. Fig. 10 shows the corresponding scalar product results for the PbPb collisions at $\sqrt{s_{\mathrm{NN}}} = 2.76\,\mathrm{TeV}$ with $\eta_{\mathrm{C}} = 0$ (top) and $= \eta_{\mathrm{ROI}}$ (bottom). The v_3 values are found to increase with increasing $N_{\rm trk}^{\rm offline}$ for both systems, as previously observed in Ref. [38]. However, contrary to what is found for the v_2 coefficients, the v_3 values are very similar for the pPb and PbPb systems in a given $N_{\rm trk}^{\rm offline}$ range.

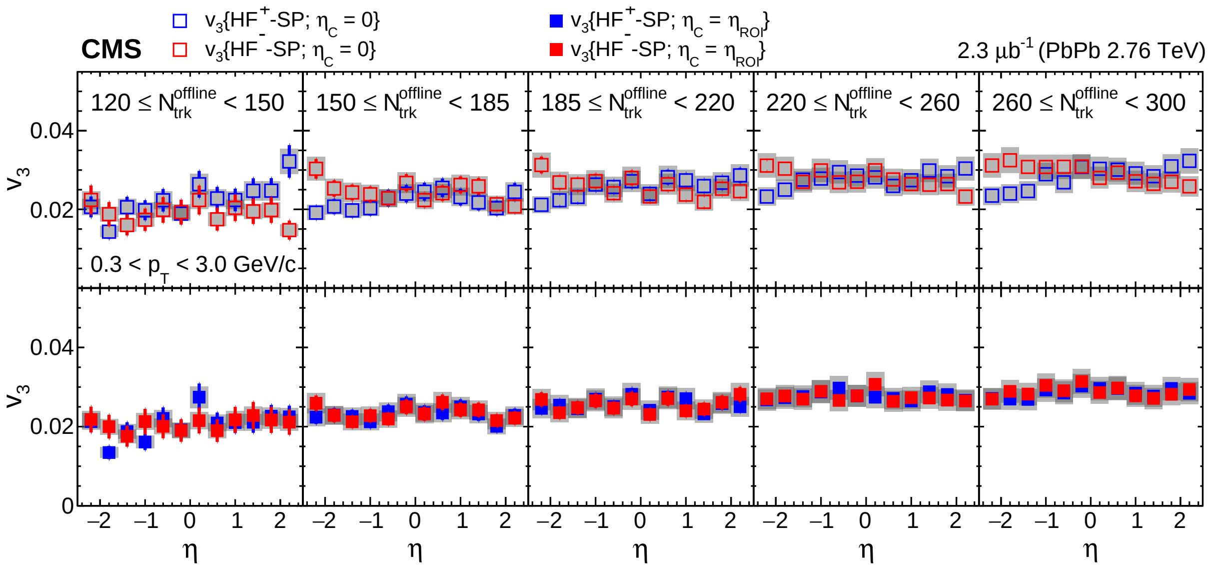

Figure 10: (Color online) (Top) The v_3 values from the scalar product method for PbPb collisions at $\sqrt{s_{\rm NN}} = 2.76$ TeV with $\eta_{\rm C} = 0$. (Bottom) Same, but with $\eta_{\rm C} = \eta_{\rm ROI}$. The notations $\rm HF^+$ and $\rm HF^-$ indicate the pseudorapidity side of the reference event plane. Pseudorapidities are given in the laboratory frame. Systematic uncertainties are indicated by the grey boxes.

In order to show the system dependence of v_2 and v_3 more directly, Fig. 11 shows scalar product results with $\eta_{\rm C} = \eta_{\rm ROI}$ for both the pPb and PbPb systems. The v_3 values, believed to result almost entirely from initial geometry fluctuations, are almost the same for the two systems. The v_2 values are still likely to reflect the lenticular shape of the collision geometry in the PbPb system, leading to larger v_2 coefficients than seen for the pPb system. The PbPb v_2 values are also found to increase with increasing event activity, reflecting the additional contribution of the changing collision overlap geometry.

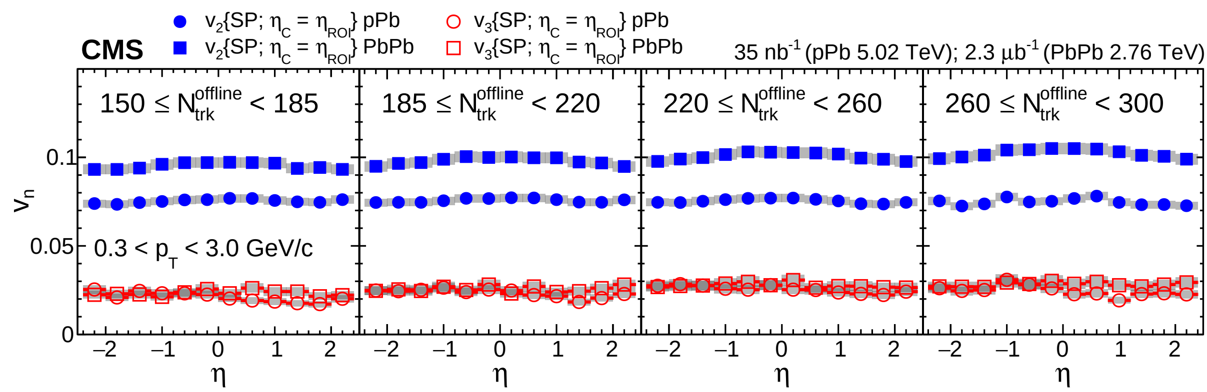

Figure 11: (Color online) The v_2 and v_3 values for pPb (PbPb) collisions at $\sqrt{s_{\rm NN}} = 5.02(2.76)$ TeV with $\eta_{\rm C} = \eta_{\rm ROI}$. The $v_n\{\rm SP\}$ results are based on the furthest HF event plane in pseudorapidity. Pseudorapidities are given in the laboratory frame. Systematic uncertainties are indicated by the grey boxes.

6 Summary

The pseudorapidity and transverse momentum dependencies of the elliptic flow v_2 coefficient are presented for pPb collisions at $\sqrt{s_{_{\mathrm{NN}}}} = 5.02\,\mathrm{TeV}$ and for peripheral PbPb collisions at $\sqrt{s_{_{\mathrm{NN}}}} = 2.76\,\mathrm{TeV}$ based on scalar product, multiparticle cumulant, and Lee–Yang zeros analyses. The data are obtained using the CMS detector. The η dependence of the triangular flow v_3 coefficient is also presented based on the scalar product analysis. For the first time, p_{T}- and η-dependent cumulant results are presented based on 6- and 8-particle correlations. The results provide detailed information for the theoretical understanding of the initial state effect and final state evolution mechanism.

All methods lead to a similar η dependence for the v_2 harmonic across the pseudorapidity range studied. The scalar product results are consistently higher than the corresponding multiparticle correlation behavior, with the $v_2\{4\}$, $v_2\{6\}$, $v_2\{8\}$, and $v_2\{\mathrm{LYZ}\}$ having comparable magnitude. An analysis of fluctuations suggests their greater influence in the system formed in pPb as compared to that in the PbPb collisions. No significant pseudorapidity dependence is found for the fluctuation component, although there is a small increase in the level of the fluctuations with increasing $N_{\mathrm{trk}}^{\mathrm{offline}}$ in both the pPb and PbPb systems. The boost invariance indicated by the decorrelation-corrected results confirms that the flow signal develops very early in the collision and thus reflects the initial-state geometry.

A method is presented to account for the possible decorrelation of the event plane angle with an increasing η gap between two regions of pseudorapidity. The results suggest that most of the η dependence observed using the different methods might be a consequence of the decorrelation effect. Earlier results exploring the η dependence of elliptic flow in heavy ion collisions may need to be reassessed based on the presence of such decorrelation effects.

Only a small difference is found for the v_2 coefficients on the Pb- and p-going sides for the pPb collisions once decorrelation effects are considered. This is in contrast to a previous study, in which the decorrelation effects were not considered and where a larger v_2 value was found on the Pb-going side. If the decorrelation effects are not considered, as is the case with the current cumulant, LYZ, and scalar product analysis with $\eta_{\mathrm{C}} = 0$, good agreement is found with the previous results. When decorrelation effects are considered, there appears to be very little longitudinal dependence of the flow coefficients near midrapidity.

The yield-weighted v_2 results of pPb and PbPb collisions at comparable values of $N_{\mathrm{trk}}^{\mathrm{offline}}$ show a similar η dependence, with the heavier system values being about 20% higher than found for pPb collisions. No significant difference is observed for the PbPb v_3 values as compared to pPb collisions, suggesting that the v_3 results are solely a consequence of fluctuations in the initial-state participant geometry.

Acknowledgments

We congratulate our colleagues in the CERN accelerator departments for the excellent performance of the LHC and thank the technical and administrative staffs at CERN and at other CMS institutes for their contributions to the success of the CMS effort. In addition, we gratefully acknowledge the computing centers and personnel of the Worldwide LHC Computing Grid for delivering so effectively the computing infrastructure essential to our analyses. Finally, we acknowledge the enduring support for the construction and operation of the LHC and the CMS detector provided by the following funding agencies: BMWFW and FWF (Austria); FNRS and FWO (Belgium); CNPq, CAPES, FAPERJ, and FAPESP (Brazil); MES (Bulgaria);

CERN; CAS, MoST, and NSFC (China); COLCIENCIAS (Colombia); MSES and CSF (Croatia); RPF (Cyprus); SENESCYT (Ecuador); MoER, ERC IUT, and ERDF (Estonia); Academy of Finland, MEC, and HIP (Finland); CEA and CNRS/IN2P3 (France); BMBF, DFG, and HGF (Germany); GSRT (Greece); OTKA and NIH (Hungary); DAE and DST (India); IPM (Iran); SFI (Ireland); INFN (Italy); MSIP and NRF (Republic of Korea); LAS (Lithuania); MOE and UM (Malaysia); BUAP, CINVESTAV, CONACYT, LNS, SEP, and UASLP-FAI (Mexico); MBIE (New Zealand); PAEC (Pakistan); MSHE and NSC (Poland); FCT (Portugal); JINR (Dubna); MON, RosAtom, RAS, RFBR and RAEP (Russia); MESTD (Serbia); SEIDI, CPAN, PCTI and FEDER (Spain); Swiss Funding Agencies (Switzerland); MST (Taipei); ThEPCenter, IPST, STAR, and NSTDA (Thailand); TUBITAK and TAEK (Turkey); NASU and SFFR (Ukraine); STFC (United Kingdom); DOE and NSF (USA).

Individuals have received support from the Marie-Curie program and the European Research Council and Horizon 2020 Grant, contract No. 675440 (European Union); the Leventis Foundation; the A. P. Sloan Foundation; the Alexander von Humboldt Foundation; the Belgian Federal Science Policy Office; the Fonds pour la Formation à la Recherche dans l'Industrie et dans l'Agriculture (FRIA-Belgium); the Agentschap voor Innovatie door Wetenschap en Technologie (IWT-Belgium); the Ministry of Education, Youth and Sports (MEYS) of the Czech Republic; the Council of Science and Industrial Research, India; the HOMING PLUS program of the Foundation for Polish Science, cofinanced from European Union, Regional Development Fund, the Mobility Plus program of the Ministry of Science and Higher Education, the National Science Center (Poland), contracts Harmonia 2014/14/M/ST2/00428, Opus 2014/13/B/ST2/02543, 2014/15/B/ST2/03998, and 2015/19/B/ST2/02861, Sonata-bis 2012/07/E/ST2/01406; the National Priorities Research Program by Qatar National Research Fund; the Programa Severo Ochoa del Principado de Asturias; the Thalis and Aristeia programs cofinanced by EU-ESF and the Greek NSRF; the Rachadapisek Sompot Fund for Postdoctoral Fellowship, Chulalongkorn University and the Chulalongkorn Academic into Its 2nd Century Project Advancement Project (Thailand); the Welch Foundation, contract C-1845; and the Weston Havens Foundation (USA).

References

[1] BRAHMS Collaboration, "Quark gluon plasma and color glass condensate at RHIC? The Perspective from the BRAHMS experiment", *Nucl. Phys. A* **757** (2005) 1, doi:10.1016/j.nuclphysa.2005.02.130, arXiv:nucl-ex/0410020.

[2] PHENIX Collaboration, "Formation of dense partonic matter in relativistic nucleus-nucleus collisions at RHIC: Experimental evaluation by the PHENIX collaboration", *Nucl. Phys. A* **757** (2005) 184, doi:10.1016/j.nuclphysa.2005.03.086, arXiv:nucl-ex/0410003.

[3] PHOBOS Collaboration, "The PHOBOS perspective on discoveries at RHIC", *Nucl. Phys. A* **757** (2005) 28, doi:10.1016/j.nuclphysa.2005.03.084, arXiv:nucl-ex/0410022.

[4] STAR Collaboration, "Experimental and theoretical challenges in the search for the quark gluon plasma: The STAR Collaboration's critical assessment of the evidence from RHIC collisions", *Nucl. Phys. A* **757** (2005) 102, doi:10.1016/j.nuclphysa.2005.03.085, arXiv:nucl-ex/0501009.

[5] ATLAS Collaboration, "Observation of a centrality-dependent dijet asymmetry in Lead-Lead collisions at $\sqrt{s_{\mathrm{NN}}} = 2.76$ TeV with the ATLAS detector at the LHC", *Phys.*

Rev. Lett. **105** (2010) 252303, doi:10.1103/PhysRevLett.105.252303, arXiv:1011.6182.

[6] CMS Collaboration, "Observation and studies of jet quenching in PbPb collisions at $\sqrt{s_{NN}} = 2.76$ TeV", *Phys. Rev. C* **84** (2011) 024906, doi:10.1103/PhysRevC.84.024906, arXiv:1102.1957.

[7] S. Voloshin and Y. Zhang, "Flow study in relativistic nuclear collisions by Fourier expansion of azimuthal particle distributions", *Z. Phys. C* **70** (1996) 665, doi:10.1007/s002880050141, arXiv:hep-ph/9407282.

[8] B. Alver and G. Roland, "Collision geometry fluctuations and triangular flow in heavy-ion collisions", *Phys. Rev. C* **81** (2010) 054905, doi:10.1103/PhysRevC.81.054905, arXiv:1003.0194. [Erratum: doi:10.1103/PhysRevC.82.039903].

[9] B. H. Alver, C. Gombeaud, M. Luzum, and J.-Y. Ollitrault, "Triangular flow in hydrodynamics and transport theory", *Phys. Rev. C* **82** (2010) 034913, doi:10.1103/PhysRevC.82.034913, arXiv:1007.5469.

[10] B. Schenke, S. Jeon, and C. Gale, "Elliptic and triangular flow in event-by-event (3+1)D viscous hydrodynamics", *Phys. Rev. Lett.* **106** (2011) 042301, doi:10.1103/PhysRevLett.106.042301, arXiv:1009.3244.

[11] Z. Qiu, C. Shen, and U. Heinz, "Hydrodynamic elliptic and triangular flow in Pb-Pb collisions at $\sqrt{s_{NN}} = 2.76$A TeV", *Phys. Lett. B* **707** (2012) 151, doi:10.1016/j.physletb.2011.12.041, arXiv:1110.3033.

[12] STAR Collaboration, "Distributions of charged hadrons associated with high transverse momentum particles in pp and Au+Au collisions at $\sqrt{s_{NN}} = 200$ GeV", *Phys. Rev. Lett.* **95** (2005) 152301, doi:10.1103/PhysRevLett.95.152301, arXiv:nucl-ex/0501016.

[13] PHOBOS Collaboration, "High transverse momentum triggered correlations over a large pseudorapidity acceptance in Au+Au collisions at $\sqrt{s_{NN}} = 200$ GeV", *Phys. Rev. Lett.* **104** (2010) 062301, doi:10.1103/PhysRevLett.104.062301, arXiv:0903.2811.

[14] STAR Collaboration, "Di-hadron correlations with identified leading hadrons in 200 GeV Au+Au and d+Au collisions at STAR", *Phys. Lett. B* **751** (2015) 233, doi:10.1016/j.physletb.2015.10.037, arXiv:1410.3524.

[15] STAR Collaboration, "Three-particle coincidence of the long range pseudorapidity correlation in high energy nucleus-nucleus collisions", *Phys. Rev. Lett.* **105** (2010) 022301, doi:10.1103/PhysRevLett.105.022301, arXiv:0912.3977.

[16] CMS Collaboration, "Long-range and short-range dihadron angular correlations in central PbPb collisions at a nucleon-nucleon center of mass energy of 2.76 TeV", *JHEP* **07** (2011) 076, doi:10.1007/JHEP07(2011)076, arXiv:1105.2438.

[17] ALICE Collaboration, "Harmonic decomposition of two particle angular correlations in Pb-Pb collisions at $\sqrt{s_{NN}} = 2.76$ TeV", *Phys. Lett. B* **708** (2012) 249, doi:10.1016/j.physletb.2012.01.060, arXiv:1109.2501.

[18] CMS Collaboration, "Centrality dependence of dihadron correlations and azimuthal anisotropy harmonics in PbPb collisions at $\sqrt{s_{NN}} = 2.76$ TeV", *Eur. Phys. J. C* **72** (2012) 72, doi:10.1140/epjc/s10052-012-2012-3, arXiv:1201.3158.

[19] ATLAS Collaboration, "Measurement of the azimuthal anisotropy for charged particle production in $\sqrt{s_{NN}} = 2.76$ TeV lead-lead collisions with the ATLAS detector", *Phys. Rev. C* **86** (2012) 014907, doi:10.1103/PhysRevC.86.014907, arXiv:1203.3087.

[20] J. Y. Ollitrault, "Anisotropy as a signature of transverse collective flow", *Phys. Rev. D* **46** (1992) 229, doi:10.1103/PhysRevD.46.229.

[21] W. Reisdorf and H. G. Ritter, "Collective flow in heavy-ion collisions", *Ann. Rev. Nucl. Part. Sci.* **47** (1997) 663, doi:10.1146/annurev.nucl.47.1.663.

[22] C. Gale, S. Jeon, and B. Schenke, "Hydrodynamic modeling of heavy-ion collisions", *Int. J. Mod. Phys. A* **28** (2013) 1340011, doi:10.1142/S0217751X13400113, arXiv:1301.5893.

[23] CMS Collaboration, "Observation of long-range near-side angular correlations in proton-proton collisions at the LHC", *JHEP* **09** (2010) 091, doi:10.1007/JHEP09(2010)091, arXiv:1009.4122.

[24] ATLAS Collaboration, "Observation of Long-Range Elliptic Azimuthal Anisotropies in $\sqrt{s} = 13$ and 2.76 TeV pp Collisions with the ATLAS Detector", *Phys. Rev. Lett.* **116** (2016) 172301, doi:10.1103/PhysRevLett.116.172301, arXiv:1509.04776.

[25] CMS Collaboration, "Measurement of long-range near-side two-particle angular correlations in pp collisions at $\sqrt{s} = 13$ TeV", *Phys. Rev. Lett.* **116** (2016) 172302, doi:10.1103/PhysRevLett.116.172302, arXiv:1510.03068.

[26] CMS Collaboration, "Evidence for collectivity in pp collisions at the LHC", *Phys. Lett. B* **765** (2017) 193, doi:10.1016/j.physletb.2016.12.009, arXiv:1606.06198.

[27] ATLAS Collaboration, "Measurements of long-range azimuthal anisotropies and associated Fourier coefficients for pp collisions at $\sqrt{s} = 5.02$ and 13 TeV and p+Pb collisions at $\sqrt{s_{NN}} = 5.02$ TeV with the ATLAS detector", *Phys. Rev. C* **96** (2017) 024908, doi:10.1103/PhysRevC.96.024908, arXiv:1609.06213.

[28] CMS Collaboration, "Observation of long-range near-side angular correlations in proton-lead collisions at the LHC", *Phys. Lett. B* **718** (2013) 795, doi:10.1016/j.physletb.2012.11.025, arXiv:1210.5482.

[29] ALICE Collaboration, "Long-range angular correlations on the near and away side in p-Pb collisions at $\sqrt{s_{NN}} = 5.02$ TeV", *Phys. Lett. B* **719** (2013) 29, doi:10.1016/j.physletb.2013.01.012, arXiv:1212.2001.

[30] ATLAS Collaboration, "Observation of associated near-side and away-side long-range correlations in $\sqrt{s_{NN}} = 5.02$ TeV proton-Lead collisions with the ATLAS detector", *Phys. Rev. Lett.* **110** (2013) 182302, doi:10.1103/PhysRevLett.110.182302, arXiv:1212.5198.

[31] ATLAS Collaboration, "Measurement of long-range pseudorapidity correlations and azimuthal harmonics in $\sqrt{s_{NN}} = 5.02$ TeV proton-lead collisions with the ATLAS detector", *Phys. Rev. C* **90** (2014) 044906, doi:10.1103/PhysRevC.90.044906, arXiv:1409.1792.

[32] LHCb Collaboration, "Measurements of long-range near-side angular correlations in $\sqrt{s_{NN}} = 5$ TeV proton-lead collisions in the forward region", *Phys. Lett. B* **762** (2016) 473, doi:10.1016/j.physletb.2016.09.064, arXiv:1512.00439.

[33] PHENIX Collaboration, "Measurement of long-range angular correlations and azimuthal anisotropies in high-multiplicity p+Au collisions at $\sqrt{s_{NN}} = 200$ GeV", *Phys. Rev. C* **95** (2017) 034910, doi:10.1103/PhysRevC.95.034910, arXiv:1609.02894.

[34] PHENIX Collaboration, "Quadrupole anisotropy in dihadron azimuthal correlations in central d+Au collisions at $\sqrt{s_{NN}} = 200$ GeV", *Phys. Rev. Lett.* **111** (2013) 212301, doi:10.1103/PhysRevLett.111.212301, arXiv:1303.1794.

[35] PHENIX Collaboration, "Measurement of long-range angular correlation and quadrupole anisotropy of pions and (anti)protons in central d+Au collisions at $\sqrt{s_{NN}} = 200$ GeV", *Phys. Rev. Lett.* **114** (2015) 192301, doi:10.1103/PhysRevLett.114.192301, arXiv:1404.7461.

[36] STAR Collaboration, "Long-range pseudorapidity dihadron correlations in d+Au collisions at $\sqrt{s_{NN}} = 200$ GeV", *Phys. Lett. B* **747** (2015) 265, doi:10.1016/j.physletb.2015.05.075, arXiv:1502.07652.

[37] PHENIX Collaboration, "Measurements of elliptic and triangular flow in high-multiplicity ^{3}He+Au collisions at $\sqrt{s_{NN}} = 200$ GeV", *Phys. Rev. Lett.* **115** (2015) 142301, doi:10.1103/PhysRevLett.115.142301, arXiv:1507.06273.

[38] CMS Collaboration, "Multiplicity and transverse momentum dependence of two- and four-particle correlations in pPb and PbPb collisions", *Phys. Lett. B* **724** (2013) 213, doi:10.1016/j.physletb.2013.06.028, arXiv:1305.0609.

[39] CMS Collaboration, "Evidence for collective multiparticle correlations in p-Pb collisions", *Phys. Rev. Lett.* **115** (2015) 012301, doi:10.1103/PhysRevLett.115.012301, arXiv:1502.05382.

[40] ATLAS Collaboration, "Measurement with the ATLAS detector of multi-particle azimuthal correlations in p+Pb collisions at $\sqrt{s_{NN}} = 5.02$ TeV", *Phys. Lett. B* **725** (2013) 60, doi:10.1016/j.physletb.2013.06.057, arXiv:1303.2084.

[41] ATLAS Collaboration, "Measurement of multi-particle azimuthal correlations with the subevent cumulant method in pp and p+Pb collisions with the ATLAS detector at the LHC", (2017). arXiv:1708.03559.

[42] N. Borghini, P. M. Dinh, and J.-Y. Ollitrault, "Flow analysis from multiparticle azimuthal correlations", *Phys. Rev. C* **64** (2001) 054901, doi:10.1103/PhysRevC.64.054901, arXiv:nucl-th/0105040.

[43] ATLAS Collaboration, "Measurement of multi-particle azimuthal correlations in pp, p+Pb and low-multiplicity Pb+Pb collisions with the ATLAS detector", *Eur. Phys. J. C* **77** (2017) 428, doi:10.1140/epjc/s10052-017-4988-1, arXiv:1705.04176.

[44] PHENIX Collaboration, "Measurements of multiparticle correlations in d+Au collisions at 200, 62.4, 39, and 19.6 GeV and p+Au collisions at 200 GeV and implications for collective behavior", (2017). arXiv:1707.06108.

[45] P. Bożek and W. Broniowski, "Correlations from hydrodynamic flow in p-Pb collisions", *Phys. Lett. B* **718** (2013) 1557, doi:10.1016/j.physletb.2012.12.051, arXiv:1211.0845.

[46] P. Bożek, "Collective flow in p-Pb and d-Pb collisions at TeV energies", *Phys. Rev. C* **85** (2012) 014911, doi:10.1103/PhysRevC.85.014911, arXiv:1112.0915.

[47] R. Venugopalan and K. Dusling, "Explanation of systematics of CMS p+Pb high multiplicity di-hadron data at $\sqrt{s_{NN}} = 5.02$ TeV", *Phys. Rev. D* **87** (2013) 054014, doi:10.1103/PhysRevD.87.054014, arXiv:1211.3701.

[48] R. Venugopalan and K. Dusling, "Evidence for BFKL and saturation dynamics from dihadron spectra at the LHC", *Phys. Rev. D* **87** (2013) 051502, doi:10.1103/PhysRevD.87.051502, arXiv:1210.3890.

[49] S. Alderweireldt and P. Van Mechelen, "Obtaining the CMS ridge effect with multiparton interactions", in *Proceedings, 3rd International Workshop on Multiple Partonic Interactions at the LHC (MPI@LHC 2011)*, p. 33. Hamburg, Germany, 2012. arXiv:1203.2048. doi:10.3204/DESY-PROC-2012-03/50.

[50] L. He et al., "Anisotropic parton escape is the dominant source of azimuthal anisotropy in transport models", *Phys. Lett. B* **753** (2016) 506, doi:10.1016/j.physletb.2015.12.051, arXiv:1601.00878.

[51] A. Bilandzic, R. Snellings, and S. Voloshin, "Flow analysis with cumulants: Direct calculations", *Phys. Rev. C* **83** (2011) 044913, doi:10.1103/PhysRevC.83.044913, arXiv:1010.0233.

[52] R. S. Bhalerao, N. Borghini, and J. Y. Ollitrault, "Analysis of anisotropic flow with Lee-Yang zeroes", *Nucl. Phys. A* **727** (2003) 373, doi:10.1016/j.nuclphysa.2003.08.007, arXiv:nucl-th/0310016.

[53] STAR Collaboration, "Elliptic flow from two and four particle correlations in Au+Au collisions at $\sqrt{s_{NN}} = 130$ GeV", *Phys. Rev. C* **66** (2002) 034904, doi:10.1103/PhysRevC.66.034904, arXiv:nucl-ex/0206001.

[54] J.-Y. Ollitrault and M. Luzum, "Eliminating experimental bias in anisotropic-flow measurements of high-energy nuclear collisions", *Phys. Rev. C* **87** (2013) 044907, doi:10.1103/PhysRevC.87.044907, arXiv:1209.2323.

[55] P. Bozek, A. Bzdak, and G.-L. Ma, "Rapidity dependence of elliptic and triangular flow in proton–nucleus collisions from collective dynamics", *Phys. Lett. B* **748** (2015) 301, doi:10.1016/j.physletb.2015.06.007, arXiv:1503.03655.

[56] CMS Collaboration, "The CMS experiment at the CERN LHC", *JINST* **3** (2008) S08004, doi:10.1088/1748-0221/3/08/S08004.

[57] GEANT4 Collaboration, "GEANT4—a simulation toolkit", *Nucl. Instrum. Meth. A* **506** (2003) 250, doi:10.1016/S0168-9002(03)01368-8.

[58] S. Porteboeuf, T. Pierog, and K. Werner, "Producing Hard Processes Regarding the Complete Event: The EPOS Event Generator", (2010). arXiv:1006.2967.

[59] M. Gyulassy and X.-N. Wang, "HIJING 1.0: A Monte Carlo program for parton and particle production in high-energy hadronic and nuclear collisions", *Comput. Phys. Commun.* **83** (1994) 307, doi:10.1016/0010-4655(94)90057-4, arXiv:nucl-th/9502021.

[60] CMS Collaboration, "Description and performance of track and primary-vertex reconstruction with the CMS tracker", *JINST* **9** (2014) P10009, doi:10.1088/1748-0221/9/10/P10009, arXiv:1405.6569.

[61] CMS Collaboration, "Azimuthal anisotropy of charged particles at high transverse momenta in PbPb collisions at $\sqrt{s_{\mathrm{NN}}} = 2.76$ TeV", *Phys. Rev. Lett.* **109** (2012) 022301, doi:10.1103/PhysRevLett.109.022301, arXiv:1204.1850.

[62] CMS Collaboration, "Measurement of the elliptic anisotropy of charged particles produced in PbPb collisions at $\sqrt{s_{\mathrm{NN}}} = 2.76$ TeV", *Phys. Rev. C* **87** (2013) 014902, doi:10.1103/PhysRevC.87.014902, arXiv:1204.1409.

[63] CMS Collaboration, "Measurement of higher-order harmonic azimuthal anisotropy in PbPb collisions at $\sqrt{s_{\mathrm{NN}}} = 2.76$ TeV", *Phys. Rev. C* **89** (2014) 044906, doi:10.1103/PhysRevC.89.044906, arXiv:1310.8651.

[64] A. M. Poskanzer and S. A. Voloshin, "Methods for analyzing anisotropic flow in relativistic nuclear collisions", *Phys. Rev. C* **58** (1998) 1671, doi:10.1103/PhysRevC.58.1671, arXiv:nucl-ex/9805001.

[65] E877 Collaboration, "Proton and pion production relative to the reaction plane in Au+Au collisions at AGS energies", *Phys. Rev. C* **56** (1997) 3254, doi:10.1103/PhysRevC.56.3254, arXiv:nucl-ex/9707002.

[66] F. G. Gardim, F. Grassi, M. Luzum, and J.-Y. Ollitrault, "Breaking of factorization of two-particle correlations in hydrodynamics", *Phys. Rev. C* **87** (2013) 031901, doi:10.1103/PhysRevC.87.031901, arXiv:1211.0989.

[67] P. Bożek, W. Broniowski, and A. Olszewski, "Hydrodynamic modeling of pseudorapidity flow correlations in relativistic heavy-ion collisions and the torque effect", *Phys. Rev. C* **91** (2015) 054912, doi:10.1103/PhysRevC.91.054912, arXiv:1503.07425.

[68] U. Heinz, Z. Qiu, and C. Shen, "Fluctuating flow angles and anisotropic flow measurements", *Phys. Rev. C* **87** (2013) 034913, doi:10.1103/PhysRevC.87.034913, arXiv:1302.3535.

[69] K. Xiao, F. Liu, and F. Wang, "Event-plane decorrelation over pseudorapidity and its effect on azimuthal anisotropy measurements in relativistic heavy-ion collisions", *Phys. Rev. C* **87** (2013) 011901, doi:10.1103/PhysRevC.87.011901, arXiv:1208.1195.

[70] CMS Collaboration, "Evidence for transverse momentum and pseudorapidity dependent event plane fluctuations in PbPb and pPb collisions", *Phys. Rev. C* **92** (2015) 034911, doi:10.1103/PhysRevC.92.034911, arXiv:1503.01692.

[71] A. Bilandzic et al., "Generic framework for anisotropic flow analyses with multiparticle azimuthal correlations", *Phys. Rev. C* **89** (2014) 064904, doi:10.1103/PhysRevC.89.064904, arXiv:1312.3572.

[72] B. Alver et al., "Importance of correlations and fluctuations on the initial source eccentricity in high-energy nucleus-nucleus collisions", *Phys. Rev. C* **77** (2008) 014906, doi:10.1103/PhysRevC.77.014906, arXiv:0711.3724.

[73] J.-Y. Ollitrault, A. M. Poskanzer, and S. A. Voloshin, "Effect of flow fluctuations and nonflow on elliptic flow methods", *Phys. Rev. C* **80** (2009) 014904, doi:10.1103/PhysRevC.80.014904, arXiv:0904.2315.

[74] CMS Collaboration, "Pseudorapidity dependence of long-range two-particle correlations in pPb collisions at $\sqrt{s_{NN}} = 5.02$ TeV", *Phys. Rev. C* **96** (2017) 014915, doi:10.1103/PhysRevC.96.014915, arXiv:1604.05347.

A The CMS Collaboration

Yerevan Physics Institute, Yerevan, Armenia
A.M. Sirunyan, A. Tumasyan

Institut für Hochenergiephysik, Wien, Austria
W. Adam, F. Ambrogi, E. Asilar, T. Bergauer, J. Brandstetter, E. Brondolin, M. Dragicevic, J. Erö, M. Flechl, M. Friedl, R. Frühwirth[1], V.M. Ghete, J. Grossmann, N. Hörmann, J. Hrubec, M. Jeitler[1], A. König, I. Krätschmer, D. Liko, T. Madlener, I. Mikulec, E. Pree, D. Rabady, N. Rad, H. Rohringer, J. Schieck[1], R. Schöfbeck, M. Spanring, D. Spitzbart, J. Strauss, W. Waltenberger, J. Wittmann, C.-E. Wulz[1], M. Zarucki

Institute for Nuclear Problems, Minsk, Belarus
V. Chekhovsky, V. Mossolov, J. Suarez Gonzalez

Universiteit Antwerpen, Antwerpen, Belgium
E.A. De Wolf, X. Janssen, J. Lauwers, M. Van De Klundert, H. Van Haevermaet, P. Van Mechelen, N. Van Remortel, A. Van Spilbeeck

Vrije Universiteit Brussel, Brussel, Belgium
S. Abu Zeid, F. Blekman, J. D'Hondt, I. De Bruyn, J. De Clercq, K. Deroover, G. Flouris, S. Lowette, S. Moortgat, L. Moreels, A. Olbrechts, Q. Python, K. Skovpen, S. Tavernier, W. Van Doninck, P. Van Mulders, I. Van Parijs

Université Libre de Bruxelles, Bruxelles, Belgium
H. Brun, B. Clerbaux, G. De Lentdecker, H. Delannoy, G. Fasanella, L. Favart, R. Goldouzian, A. Grebenyuk, G. Karapostoli, T. Lenzi, J. Luetic, T. Maerschalk, A. Marinov, A. Randle-conde, T. Seva, C. Vander Velde, P. Vanlaer, D. Vannerom, R. Yonamine, F. Zenoni, F. Zhang[2]

Ghent University, Ghent, Belgium
A. Cimmino, T. Cornelis, D. Dobur, A. Fagot, M. Gul, I. Khvastunov, D. Poyraz, S. Salva, M. Tytgat, W. Verbeke, N. Zaganidis

Université Catholique de Louvain, Louvain-la-Neuve, Belgium
H. Bakhshiansohi, O. Bondu, S. Brochet, G. Bruno, A. Caudron, S. De Visscher, C. Delaere, M. Delcourt, B. Francois, A. Giammanco, A. Jafari, M. Komm, G. Krintiras, V. Lemaitre, A. Magitteri, A. Mertens, M. Musich, K. Piotrzkowski, L. Quertenmont, M. Vidal Marono, S. Wertz

Université de Mons, Mons, Belgium
N. Beliy

Centro Brasileiro de Pesquisas Fisicas, Rio de Janeiro, Brazil
W.L. Aldá Júnior, F.L. Alves, G.A. Alves, L. Brito, C. Hensel, A. Moraes, M.E. Pol, P. Rebello Teles

Universidade do Estado do Rio de Janeiro, Rio de Janeiro, Brazil
E. Belchior Batista Das Chagas, W. Carvalho, J. Chinellato[3], A. Custódio, E.M. Da Costa, G.G. Da Silveira[4], D. De Jesus Damiao, S. Fonseca De Souza, L.M. Huertas Guativa, H. Malbouisson, M. Melo De Almeida, C. Mora Herrera, L. Mundim, H. Nogima, A. Santoro, A. Sznajder, E.J. Tonelli Manganote[3], F. Torres Da Silva De Araujo, A. Vilela Pereira

Universidade Estadual Paulista [a], Universidade Federal do ABC [b], São Paulo, Brazil
S. Ahuja[a], C.A. Bernardes[a], T.R. Fernandez Perez Tomei[a], E.M. Gregores[b], P.G. Mercadante[b], C.S. Moon[a], S.F. Novaes[a], Sandra S. Padula[a], D. Romero Abad[b], J.C. Ruiz Vargas[a]

Institute for Nuclear Research and Nuclear Energy of Bulgaria Academy of Sciences
A. Aleksandrov, R. Hadjiiska, P. Iaydjiev, M. Misheva, M. Rodozov, S. Stoykova, G. Sultanov, M. Vutova

University of Sofia, Sofia, Bulgaria
A. Dimitrov, I. Glushkov, L. Litov, B. Pavlov, P. Petkov

Beihang University, Beijing, China
W. Fang[5], X. Gao[5]

Institute of High Energy Physics, Beijing, China
M. Ahmad, J.G. Bian, G.M. Chen, H.S. Chen, M. Chen, Y. Chen, C.H. Jiang, D. Leggat, Z. Liu, F. Romeo, S.M. Shaheen, A. Spiezia, J. Tao, C. Wang, Z. Wang, E. Yazgan, H. Zhang, J. Zhao

State Key Laboratory of Nuclear Physics and Technology, Peking University, Beijing, China
Y. Ban, G. Chen, Q. Li, S. Liu, Y. Mao, S.J. Qian, D. Wang, Z. Xu

Universidad de Los Andes, Bogota, Colombia
C. Avila, A. Cabrera, L.F. Chaparro Sierra, C. Florez, C.F. González Hernández, J.D. Ruiz Alvarez

University of Split, Faculty of Electrical Engineering, Mechanical Engineering and Naval Architecture, Split, Croatia
N. Godinovic, D. Lelas, I. Puljak, P.M. Ribeiro Cipriano, T. Sculac

University of Split, Faculty of Science, Split, Croatia
Z. Antunovic, M. Kovac

Institute Rudjer Boskovic, Zagreb, Croatia
V. Brigljevic, D. Ferencek, K. Kadija, B. Mesic, T. Susa

University of Cyprus, Nicosia, Cyprus
M.W. Ather, A. Attikis, G. Mavromanolakis, J. Mousa, C. Nicolaou, F. Ptochos, P.A. Razis, H. Rykaczewski

Charles University, Prague, Czech Republic
M. Finger[6], M. Finger Jr.[6]

Universidad San Francisco de Quito, Quito, Ecuador
E. Carrera Jarrin

Academy of Scientific Research and Technology of the Arab Republic of Egypt, Egyptian Network of High Energy Physics, Cairo, Egypt
A.A. Abdelalim[7,8], M.A. Mahmoud[9,10], A. Mahrous[7]

National Institute of Chemical Physics and Biophysics, Tallinn, Estonia
R.K. Dewanjee, M. Kadastik, L. Perrini, M. Raidal, A. Tiko, C. Veelken

Department of Physics, University of Helsinki, Helsinki, Finland
P. Eerola, J. Pekkanen, M. Voutilainen

Helsinki Institute of Physics, Helsinki, Finland
J. Härkönen, T. Järvinen, V. Karimäki, R. Kinnunen, T. Lampén, K. Lassila-Perini, S. Lehti, T. Lindén, P. Luukka, E. Tuominen, J. Tuominiemi, E. Tuovinen

Lappeenranta University of Technology, Lappeenranta, Finland
J. Talvitie, T. Tuuva

IRFU, CEA, Université Paris-Saclay, Gif-sur-Yvette, France
M. Besancon, F. Couderc, M. Dejardin, D. Denegri, J.L. Faure, F. Ferri, S. Ganjour, S. Ghosh, A. Givernaud, P. Gras, G. Hamel de Monchenault, P. Jarry, I. Kucher, E. Locci, M. Machet, J. Malcles, J. Rander, A. Rosowsky, M.Ö. Sahin, M. Titov

Laboratoire Leprince-Ringuet, Ecole polytechnique, CNRS/IN2P3, Université Paris-Saclay, Palaiseau, France
A. Abdulsalam, I. Antropov, S. Baffioni, F. Beaudette, P. Busson, L. Cadamuro, C. Charlot, O. Davignon, R. Granier de Cassagnac, M. Jo, S. Lisniak, A. Lobanov, M. Nguyen, C. Ochando, G. Ortona, P. Paganini, P. Pigard, S. Regnard, R. Salerno, Y. Sirois, A.G. Stahl Leiton, T. Strebler, Y. Yilmaz, A. Zabi, A. Zghiche

Université de Strasbourg, CNRS, IPHC UMR 7178, F-67000 Strasbourg, France
J.-L. Agram[11], J. Andrea, D. Bloch, J.-M. Brom, M. Buttignol, E.C. Chabert, N. Chanon, C. Collard, E. Conte[11], X. Coubez, J.-C. Fontaine[11], D. Gelé, U. Goerlach, A.-C. Le Bihan, P. Van Hove

Centre de Calcul de l'Institut National de Physique Nucleaire et de Physique des Particules, CNRS/IN2P3, Villeurbanne, France
S. Gadrat

Université de Lyon, Université Claude Bernard Lyon 1, CNRS-IN2P3, Institut de Physique Nucléaire de Lyon, Villeurbanne, France
S. Beauceron, C. Bernet, G. Boudoul, R. Chierici, D. Contardo, B. Courbon, P. Depasse, H. El Mamouni, J. Fay, L. Finco, S. Gascon, M. Gouzevitch, G. Grenier, B. Ille, F. Lagarde, I.B. Laktineh, M. Lethuillier, L. Mirabito, A.L. Pequegnot, S. Perries, A. Popov[12], V. Sordini, M. Vander Donckt, S. Viret

Georgian Technical University, Tbilisi, Georgia
T. Toriashvili[13]

Tbilisi State University, Tbilisi, Georgia
Z. Tsamalaidze[6]

RWTH Aachen University, I. Physikalisches Institut, Aachen, Germany
C. Autermann, S. Beranek, L. Feld, M.K. Kiesel, K. Klein, M. Lipinski, M. Preuten, C. Schomakers, J. Schulz, T. Verlage

RWTH Aachen University, III. Physikalisches Institut A, Aachen, Germany
A. Albert, M. Brodski, E. Dietz-Laursonn, D. Duchardt, M. Endres, M. Erdmann, S. Erdweg, T. Esch, R. Fischer, A. Güth, M. Hamer, T. Hebbeker, C. Heidemann, K. Hoepfner, S. Knutzen, M. Merschmeyer, A. Meyer, P. Millet, S. Mukherjee, M. Olschewski, K. Padeken, T. Pook, M. Radziej, H. Reithler, M. Rieger, F. Scheuch, L. Sonnenschein, D. Teyssier, S. Thüer

RWTH Aachen University, III. Physikalisches Institut B, Aachen, Germany
G. Flügge, B. Kargoll, T. Kress, A. Künsken, J. Lingemann, T. Müller, A. Nehrkorn, A. Nowack, C. Pistone, O. Pooth, A. Stahl[14]

Deutsches Elektronen-Synchrotron, Hamburg, Germany
M. Aldaya Martin, T. Arndt, C. Asawatangtrakuldee, K. Beernaert, O. Behnke, U. Behrens, A.A. Bin Anuar, K. Borras[15], V. Botta, A. Campbell, P. Connor, C. Contreras-Campana, F. Costanza, C. Diez Pardos, G. Eckerlin, D. Eckstein, T. Eichhorn, E. Eren, E. Gallo[16], J. Garay Garcia, A. Geiser, A. Gizhko, J.M. Grados Luyando, A. Grohsjean, P. Gunnellini, A. Harb, J. Hauk, M. Hempel[17], H. Jung, A. Kalogeropoulos, M. Kasemann, J. Keaveney,

C. Kleinwort, I. Korol, D. Krücker, W. Lange, A. Lelek, T. Lenz, J. Leonard, K. Lipka, W. Lohmann[17], R. Mankel, I.-A. Melzer-Pellmann, A.B. Meyer, G. Mittag, J. Mnich, A. Mussgiller, E. Ntomari, D. Pitzl, R. Placakyte, A. Raspereza, B. Roland, M. Savitskyi, P. Saxena, R. Shevchenko, S. Spannagel, N. Stefaniuk, G.P. Van Onsem, R. Walsh, Y. Wen, K. Wichmann, C. Wissing, O. Zenaiev

University of Hamburg, Hamburg, Germany
S. Bein, V. Blobel, M. Centis Vignali, A.R. Draeger, T. Dreyer, E. Garutti, D. Gonzalez, J. Haller, M. Hoffmann, A. Junkes, R. Klanner, R. Kogler, N. Kovalchuk, S. Kurz, T. Lapsien, I. Marchesini, D. Marconi, M. Meyer, M. Niedziela, D. Nowatschin, F. Pantaleo[14], T. Peiffer, A. Perieanu, C. Scharf, P. Schleper, A. Schmidt, S. Schumann, J. Schwandt, J. Sonneveld, H. Stadie, G. Steinbrück, F.M. Stober, M. Stöver, H. Tholen, D. Troendle, E. Usai, L. Vanelderen, A. Vanhoefer, B. Vormwald

Institut für Experimentelle Kernphysik, Karlsruhe, Germany
M. Akbiyik, C. Barth, S. Baur, C. Baus, J. Berger, E. Butz, R. Caspart, T. Chwalek, F. Colombo, W. De Boer, A. Dierlamm, B. Freund, R. Friese, M. Giffels, A. Gilbert, D. Haitz, F. Hartmann[14], S.M. Heindl, U. Husemann, F. Kassel[14], S. Kudella, H. Mildner, M.U. Mozer, Th. Müller, M. Plagge, G. Quast, K. Rabbertz, M. Schröder, I. Shvetsov, G. Sieber, H.J. Simonis, R. Ulrich, S. Wayand, M. Weber, T. Weiler, S. Williamson, C. Wöhrmann, R. Wolf

Institute of Nuclear and Particle Physics (INPP), NCSR Demokritos, Aghia Paraskevi, Greece
G. Anagnostou, G. Daskalakis, T. Geralis, V.A. Giakoumopoulou, A. Kyriakis, D. Loukas, I. Topsis-Giotis

National and Kapodistrian University of Athens, Athens, Greece
S. Kesisoglou, A. Panagiotou, N. Saoulidou

University of Ioánnina, Ioánnina, Greece
I. Evangelou, C. Foudas, P. Kokkas, N. Manthos, I. Papadopoulos, E. Paradas, J. Strologas, F.A. Triantis

MTA-ELTE Lendület CMS Particle and Nuclear Physics Group, Eötvös Loránd University, Budapest, Hungary
M. Csanad, N. Filipovic, G. Pasztor

Wigner Research Centre for Physics, Budapest, Hungary
G. Bencze, C. Hajdu, D. Horvath[18], F. Sikler, V. Veszpremi, G. Vesztergombi[19], A.J. Zsigmond

Institute of Nuclear Research ATOMKI, Debrecen, Hungary
N. Beni, S. Czellar, J. Karancsi[20], A. Makovec, J. Molnar, Z. Szillasi

Institute of Physics, University of Debrecen, Debrecen, Hungary
M. Bartók[19], P. Raics, Z.L. Trocsanyi, B. Ujvari

Indian Institute of Science (IISc), Bangalore, India
S. Choudhury, J.R. Komaragiri

National Institute of Science Education and Research, Bhubaneswar, India
S. Bahinipati[21], S. Bhowmik, P. Mal, K. Mandal, A. Nayak[22], D.K. Sahoo[21], N. Sahoo, S.K. Swain

Panjab University, Chandigarh, India
S. Bansal, S.B. Beri, V. Bhatnagar, U. Bhawandeep, R. Chawla, N. Dhingra, A.K. Kalsi, A. Kaur, M. Kaur, R. Kumar, P. Kumari, A. Mehta, M. Mittal, J.B. Singh, G. Walia

University of Delhi, Delhi, India
A. Bhardwaj, S. Chauhan, B.C. Choudhary, R.B. Garg, S. Keshri, A. Kumar, Ashok Kumar, S. Malhotra, M. Naimuddin, K. Ranjan, Aashaq Shah, R. Sharma, V. Sharma

Saha Institute of Nuclear Physics, HBNI, Kolkata, India
R. Bhardwaj, R. Bhattacharya, S. Bhattacharya, S. Dey, S. Dutt, S. Dutta, S. Ghosh, N. Majumdar, A. Modak, K. Mondal, S. Mukhopadhyay, S. Nandan, A. Purohit, A. Roy, D. Roy, S. Roy Chowdhury, S. Sarkar, M. Sharan, S. Thakur

Indian Institute of Technology Madras, Madras, India
P.K. Behera

Bhabha Atomic Research Centre, Mumbai, India
R. Chudasama, D. Dutta, V. Jha, V. Kumar, A.K. Mohanty[14], P.K. Netrakanti, L.M. Pant, P. Shukla, A. Topkar

Tata Institute of Fundamental Research-A, Mumbai, India
T. Aziz, S. Dugad, B. Mahakud, S. Mitra, G.B. Mohanty, B. Parida, N. Sur, B. Sutar

Tata Institute of Fundamental Research-B, Mumbai, India
S. Banerjee, S. Bhattacharya, S. Chatterjee, P. Das, M. Guchait, Sa. Jain, S. Kumar, M. Maity[23], G. Majumder, K. Mazumdar, T. Sarkar[23], N. Wickramage[24]

Indian Institute of Science Education and Research (IISER), Pune, India
S. Chauhan, S. Dube, V. Hegde, A. Kapoor, K. Kothekar, S. Pandey, A. Rane, S. Sharma

Institute for Research in Fundamental Sciences (IPM), Tehran, Iran
S. Chenarani[25], E. Eskandari Tadavani, S.M. Etesami[25], M. Khakzad, M. Mohammadi Najafabadi, M. Naseri, S. Paktinat Mehdiabadi[26], F. Rezaei Hosseinabadi, B. Safarzadeh[27], M. Zeinali

University College Dublin, Dublin, Ireland
M. Felcini, M. Grunewald

INFN Sezione di Bari [a], Università di Bari [b], Politecnico di Bari [c], Bari, Italy
M. Abbrescia[a,b], C. Calabria[a,b], C. Caputo[a,b], A. Colaleo[a], D. Creanza[a,c], L. Cristella[a,b], N. De Filippis[a,c], M. De Palma[a,b], L. Fiore[a], G. Iaselli[a,c], G. Maggi[a,c], M. Maggi[a], G. Miniello[a,b], S. My[a,b], S. Nuzzo[a,b], A. Pompili[a,b], G. Pugliese[a,c], R. Radogna[a,b], A. Ranieri[a], G. Selvaggi[a,b], A. Sharma[a], L. Silvestris[a,14], R. Venditti[a], P. Verwilligen[a]

INFN Sezione di Bologna [a], Università di Bologna [b], Bologna, Italy
G. Abbiendi[a], C. Battilana, D. Bonacorsi[a,b], S. Braibant-Giacomelli[a,b], L. Brigliadori[a,b], R. Campanini[a,b], P. Capiluppi[a,b], A. Castro[a,b], F.R. Cavallo[a], S.S. Chhibra[a,b], G. Codispoti[a,b], M. Cuffiani[a,b], G.M. Dallavalle[a], F. Fabbri[a], A. Fanfani[a,b], D. Fasanella[a,b], P. Giacomelli[a], L. Guiducci[a,b], S. Marcellini[a], G. Masetti[a], F.L. Navarria[a,b], A. Perrotta[a], A.M. Rossi[a,b], T. Rovelli[a,b], G.P. Siroli[a,b], N. Tosi[a,b,14]

INFN Sezione di Catania [a], Università di Catania [b], Catania, Italy
S. Albergo[a,b], S. Costa[a,b], A. Di Mattia[a], F. Giordano[a,b], R. Potenza[a,b], A. Tricomi[a,b], C. Tuve[a,b]

INFN Sezione di Firenze [a], Università di Firenze [b], Firenze, Italy
G. Barbagli[a], K. Chatterjee[a,b], V. Ciulli[a,b], C. Civinini[a], R. D'Alessandro[a,b], E. Focardi[a,b], P. Lenzi[a,b], M. Meschini[a], S. Paoletti[a], L. Russo[a,28], G. Sguazzoni[a], D. Strom[a], L. Viliani[a,b,14]

INFN Laboratori Nazionali di Frascati, Frascati, Italy
L. Benussi, S. Bianco, F. Fabbri, D. Piccolo, F. Primavera[14]

INFN Sezione di Genova [a], Università di Genova [b], Genova, Italy
V. Calvelli[a,b], F. Ferro[a], E. Robutti[a], S. Tosi[a,b]

INFN Sezione di Milano-Bicocca [a], Università di Milano-Bicocca [b], Milano, Italy
L. Brianza[a,b], F. Brivio[a,b], V. Ciriolo[a,b], M.E. Dinardo[a,b], S. Fiorendi[a,b], S. Gennai[a], A. Ghezzi[a,b], P. Govoni[a,b], M. Malberti[a,b], S. Malvezzi[a], R.A. Manzoni[a,b], D. Menasce[a], L. Moroni[a], M. Paganoni[a,b], K. Pauwels[a,b], D. Pedrini[a], S. Pigazzini[a,b,29], S. Ragazzi[a,b], T. Tabarelli de Fatis[a,b]

INFN Sezione di Napoli [a], Università di Napoli 'Federico II' [b], Napoli, Italy, Università della Basilicata [c], Potenza, Italy, Università G. Marconi [d], Roma, Italy
S. Buontempo[a], N. Cavallo[a,c], S. Di Guida[a,d,14], F. Fabozzi[a,c], F. Fienga[a,b], A.O.M. Iorio[a,b], W.A. Khan[a], L. Lista[a], S. Meola[a,d,14], P. Paolucci[a,14], C. Sciacca[a,b], F. Thyssen[a]

INFN Sezione di Padova [a], Università di Padova [b], Padova, Italy, Università di Trento [c], Trento, Italy
P. Azzi[a,14], N. Bacchetta[a], L. Benato[a,b], D. Bisello[a,b], A. Boletti[a,b], R. Carlin[a,b], P. Checchia[a], M. Dall'Osso[a,b], T. Dorigo[a], U. Dosselli[a], F. Gasparini[a,b], U. Gasparini[a,b], A. Gozzelino[a], M. Gulmini[a,30], S. Lacaprara[a], M. Margoni[a,b], G. Maron[a,30], A.T. Meneguzzo[a,b], N. Pozzobon[a,b], P. Ronchese[a,b], R. Rossin[a,b], E. Torassa[a], S. Ventura[a], M. Zanetti[a,b], P. Zotto[a,b], G. Zumerle[a,b]

INFN Sezione di Pavia [a], Università di Pavia [b], Pavia, Italy
A. Braghieri[a], F. Fallavollita[a,b], A. Magnani[a,b], P. Montagna[a,b], S.P. Ratti[a,b], V. Re[a], M. Ressegotti, C. Riccardi[a,b], P. Salvini[a], I. Vai[a,b], P. Vitulo[a,b]

INFN Sezione di Perugia [a], Università di Perugia [b], Perugia, Italy
L. Alunni Solestizi[a,b], G.M. Bilei[a], D. Ciangottini[a,b], L. Fanò[a,b], P. Lariccia[a,b], R. Leonardi[a,b], G. Mantovani[a,b], V. Mariani[a,b], M. Menichelli[a], A. Saha[a], A. Santocchia[a,b], D. Spiga

INFN Sezione di Pisa [a], Università di Pisa [b], Scuola Normale Superiore di Pisa [c], Pisa, Italy
K. Androsov[a], P. Azzurri[a,14], G. Bagliesi[a], J. Bernardini[a], T. Boccali[a], L. Borrello, R. Castaldi[a], M.A. Ciocci[a,b], R. Dell'Orso[a], G. Fedi[a], A. Giassi[a], M.T. Grippo[a,28], F. Ligabue[a,c], T. Lomtadze[a], L. Martini[a,b], A. Messineo[a,b], F. Palla[a], A. Rizzi[a,b], A. Savoy-Navarro[a,31], P. Spagnolo[a], R. Tenchini[a], G. Tonelli[a,b], A. Venturi[a], P.G. Verdini[a]

INFN Sezione di Roma [a], Sapienza Università di Roma [b], Rome, Italy
L. Barone[a,b], F. Cavallari[a], M. Cipriani[a,b], N. Daci[a], D. Del Re[a,b,14], M. Diemoz[a], S. Gelli[a,b], E. Longo[a,b], F. Margaroli[a,b], B. Marzocchi[a,b], P. Meridiani[a], G. Organtini[a,b], R. Paramatti[a,b], F. Preiato[a,b], S. Rahatlou[a,b], C. Rovelli[a], F. Santanastasio[a,b]

INFN Sezione di Torino [a], Università di Torino [b], Torino, Italy, Università del Piemonte Orientale [c], Novara, Italy
N. Amapane[a,b], R. Arcidiacono[a,c,14], S. Argiro[a,b], M. Arneodo[a,c], N. Bartosik[a], R. Bellan[a,b], C. Biino[a], N. Cartiglia[a], F. Cenna[a,b], M. Costa[a,b], R. Covarelli[a,b], A. Degano[a,b], N. Demaria[a], B. Kiani[a,b], C. Mariotti[a], S. Maselli[a], E. Migliore[a,b], V. Monaco[a,b], E. Monteil[a,b], M. Monteno[a], M.M. Obertino[a,b], L. Pacher[a,b], N. Pastrone[a], M. Pelliccioni[a], G.L. Pinna Angioni[a,b], F. Ravera[a,b], A. Romero[a,b], M. Ruspa[a,c], R. Sacchi[a,b], K. Shchelina[a,b], V. Sola[a], A. Solano[a,b], A. Staiano[a], P. Traczyk[a,b]

INFN Sezione di Trieste [a], Università di Trieste [b], Trieste, Italy
S. Belforte[a], M. Casarsa[a], F. Cossutti[a], G. Della Ricca[a,b], A. Zanetti[a]

Kyungpook National University, Daegu, Korea
D.H. Kim, G.N. Kim, M.S. Kim, J. Lee, S. Lee, S.W. Lee, Y.D. Oh, S. Sekmen, D.C. Son, Y.C. Yang

Chonbuk National University, Jeonju, Korea
A. Lee

Chonnam National University, Institute for Universe and Elementary Particles, Kwangju, Korea
H. Kim, D.H. Moon, G. Oh

Hanyang University, Seoul, Korea
J.A. Brochero Cifuentes, J. Goh, T.J. Kim

Korea University, Seoul, Korea
S. Cho, S. Choi, Y. Go, D. Gyun, S. Ha, B. Hong, Y. Jo, Y. Kim, K. Lee, K.S. Lee, S. Lee, J. Lim, S.K. Park, Y. Roh

Seoul National University, Seoul, Korea
J. Almond, J. Kim, J.S. Kim, H. Lee, K. Lee, K. Nam, S.B. Oh, B.C. Radburn-Smith, S.h. Seo, U.K. Yang, H.D. Yoo, G.B. Yu

University of Seoul, Seoul, Korea
M. Choi, H. Kim, J.H. Kim, J.S.H. Lee, I.C. Park, G. Ryu

Sungkyunkwan University, Suwon, Korea
Y. Choi, C. Hwang, J. Lee, I. Yu

Vilnius University, Vilnius, Lithuania
V. Dudenas, A. Juodagalvis, J. Vaitkus

National Centre for Particle Physics, Universiti Malaya, Kuala Lumpur, Malaysia
I. Ahmed, Z.A. Ibrahim, M.A.B. Md Ali[32], F. Mohamad Idris[33], W.A.T. Wan Abdullah, M.N. Yusli, Z. Zolkapli

Centro de Investigacion y de Estudios Avanzados del IPN, Mexico City, Mexico
H. Castilla-Valdez, E. De La Cruz-Burelo, I. Heredia-De La Cruz[34], R. Lopez-Fernandez, J. Mejia Guisao, A. Sanchez-Hernandez

Universidad Iberoamericana, Mexico City, Mexico
S. Carrillo Moreno, C. Oropeza Barrera, F. Vazquez Valencia

Benemerita Universidad Autonoma de Puebla, Puebla, Mexico
I. Pedraza, H.A. Salazar Ibarguen, C. Uribe Estrada

Universidad Autónoma de San Luis Potosí, San Luis Potosí, Mexico
A. Morelos Pineda

University of Auckland, Auckland, New Zealand
D. Krofcheck

University of Canterbury, Christchurch, New Zealand
P.H. Butler

National Centre for Physics, Quaid-I-Azam University, Islamabad, Pakistan
A. Ahmad, M. Ahmad, Q. Hassan, H.R. Hoorani, A. Saddique, M.A. Shah, M. Shoaib, M. Waqas

National Centre for Nuclear Research, Swierk, Poland
H. Bialkowska, M. Bluj, B. Boimska, T. Frueboes, M. Górski, M. Kazana, K. Nawrocki, K. Romanowska-Rybinska, M. Szleper, P. Zalewski

Institute of Experimental Physics, Faculty of Physics, University of Warsaw, Warsaw, Poland
K. Bunkowski, A. Byszuk[35], K. Doroba, A. Kalinowski, M. Konecki, J. Krolikowski, M. Misiura, M. Olszewski, A. Pyskir, M. Walczak

Laboratório de Instrumentação e Física Experimental de Partículas, Lisboa, Portugal
P. Bargassa, C. Beirão Da Cruz E Silva, B. Calpas, A. Di Francesco, P. Faccioli, M. Gallinaro, J. Hollar, N. Leonardo, L. Lloret Iglesias, M.V. Nemallapudi, J. Seixas, O. Toldaiev, D. Vadruccio, J. Varela

Joint Institute for Nuclear Research, Dubna, Russia
S. Afanasiev, P. Bunin, M. Gavrilenko, I. Golutvin, I. Gorbunov, A. Kamenev, V. Karjavin, A. Lanev, A. Malakhov, V. Matveev[36,37], V. Palichik, V. Perelygin, S. Shmatov, S. Shulha, N. Skatchkov, V. Smirnov, N. Voytishin, A. Zarubin

Petersburg Nuclear Physics Institute, Gatchina (St. Petersburg), Russia
Y. Ivanov, V. Kim[38], E. Kuznetsova[39], P. Levchenko, V. Murzin, V. Oreshkin, I. Smirnov, V. Sulimov, L. Uvarov, S. Vavilov, A. Vorobyev

Institute for Nuclear Research, Moscow, Russia
Yu. Andreev, A. Dermenev, S. Gninenko, N. Golubev, A. Karneyeu, M. Kirsanov, N. Krasnikov, A. Pashenkov, D. Tlisov, A. Toropin

Institute for Theoretical and Experimental Physics, Moscow, Russia
V. Epshteyn, V. Gavrilov, N. Lychkovskaya, V. Popov, I. Pozdnyakov, G. Safronov, A. Spiridonov, A. Stepennov, M. Toms, E. Vlasov, A. Zhokin

Moscow Institute of Physics and Technology, Moscow, Russia
T. Aushev, A. Bylinkin[37]

National Research Nuclear University 'Moscow Engineering Physics Institute' (MEPhI), Moscow, Russia
R. Chistov[40], D. Philippov, S. Polikarpov

P.N. Lebedev Physical Institute, Moscow, Russia
V. Andreev, M. Azarkin[37], I. Dremin[37], M. Kirakosyan, A. Terkulov

Skobeltsyn Institute of Nuclear Physics, Lomonosov Moscow State University, Moscow, Russia
A. Baskakov, A. Belyaev, E. Boos, A. Ershov, A. Gribushin, A. Kaminskiy[41], O. Kodolova, V. Korotkikh, I. Lokhtin, I. Miagkov, S. Obraztsov, S. Petrushanko, V. Savrin, A. Snigirev, I. Vardanyan

Novosibirsk State University (NSU), Novosibirsk, Russia
V. Blinov[42], D. Shtol[42], Y.Skovpen[42]

State Research Center of Russian Federation, Institute for High Energy Physics, Protvino, Russia
I. Azhgirey, I. Bayshev, S. Bitioukov, D. Elumakhov, V. Kachanov, A. Kalinin, D. Konstantinov, V. Krychkine, V. Petrov, R. Ryutin, A. Sobol, S. Troshin, N. Tyurin, A. Uzunian, A. Volkov

University of Belgrade, Faculty of Physics and Vinca Institute of Nuclear Sciences, Belgrade, Serbia
P. Adzic[43], P. Cirkovic, D. Devetak, M. Dordevic, J. Milosevic, V. Rekovic

Centro de Investigaciones Energéticas Medioambientales y Tecnológicas (CIEMAT), Madrid, Spain
J. Alcaraz Maestre, A. Álvarez Fernández, M. Barrio Luna, M. Cerrada, N. Colino, B. De La Cruz, A. Delgado Peris, A. Escalante Del Valle, C. Fernandez Bedoya, J.P. Fernández Ramos, J. Flix, M.C. Fouz, P. Garcia-Abia, O. Gonzalez Lopez, S. Goy Lopez, J.M. Hernandez, M.I. Josa, A. Pérez-Calero Yzquierdo, J. Puerta Pelayo, A. Quintario Olmeda, I. Redondo, L. Romero, M.S. Soares

Universidad Autónoma de Madrid, Madrid, Spain
C. Albajar, J.F. de Trocóniz, M. Missiroli, D. Moran

Universidad de Oviedo, Oviedo, Spain
J. Cuevas, C. Erice, J. Fernandez Menendez, I. Gonzalez Caballero, J.R. González Fernández, E. Palencia Cortezon, S. Sanchez Cruz, I. Suárez Andrés, P. Vischia, J.M. Vizan Garcia

Instituto de Física de Cantabria (IFCA), CSIC-Universidad de Cantabria, Santander, Spain
I.J. Cabrillo, A. Calderon, B. Chazin Quero, E. Curras, M. Fernandez, J. Garcia-Ferrero, G. Gomez, A. Lopez Virto, J. Marco, C. Martinez Rivero, P. Martinez Ruiz del Arbol, F. Matorras, J. Piedra Gomez, T. Rodrigo, A. Ruiz-Jimeno, L. Scodellaro, N. Trevisani, I. Vila, R. Vilar Cortabitarte

CERN, European Organization for Nuclear Research, Geneva, Switzerland
D. Abbaneo, E. Auffray, P. Baillon, A.H. Ball, D. Barney, M. Bianco, P. Bloch, A. Bocci, C. Botta, T. Camporesi, R. Castello, M. Cepeda, G. Cerminara, E. Chapon, Y. Chen, D. d'Enterria, A. Dabrowski, V. Daponte, A. David, M. De Gruttola, A. De Roeck, E. Di Marco[44], M. Dobson, B. Dorney, T. du Pree, M. Dünser, N. Dupont, A. Elliott-Peisert, P. Everaerts, G. Franzoni, J. Fulcher, W. Funk, D. Gigi, K. Gill, F. Glege, D. Gulhan, S. Gundacker, M. Guthoff, P. Harris, J. Hegeman, V. Innocente, P. Janot, O. Karacheban[17], J. Kieseler, H. Kirschenmann, V. Knünz, A. Kornmayer[14], M.J. Kortelainen, M. Krammer[1], C. Lange, P. Lecoq, C. Lourenço, M.T. Lucchini, L. Malgeri, M. Mannelli, A. Martelli, F. Meijers, J.A. Merlin, S. Mersi, E. Meschi, P. Milenovic[45], F. Moortgat, M. Mulders, H. Neugebauer, S. Orfanelli, L. Orsini, L. Pape, E. Perez, M. Peruzzi, A. Petrilli, G. Petrucciani, A. Pfeiffer, M. Pierini, A. Racz, T. Reis, G. Rolandi[46], M. Rovere, H. Sakulin, J.B. Sauvan, C. Schäfer, C. Schwick, M. Seidel, M. Selvaggi, A. Sharma, P. Silva, P. Sphicas[47], J. Steggemann, M. Stoye, M. Tosi, D. Treille, A. Triossi, A. Tsirou, V. Veckalns[48], G.I. Veres[19], M. Verweij, N. Wardle, W.D. Zeuner

Paul Scherrer Institut, Villigen, Switzerland
W. Bertl[†], K. Deiters, W. Erdmann, R. Horisberger, Q. Ingram, H.C. Kaestli, D. Kotlinski, U. Langenegger, T. Rohe, S.A. Wiederkehr

ETH Zurich - Institute for Particle Physics and Astrophysics (IPA), Zurich, Switzerland
F. Bachmair, L. Bäni, P. Berger, L. Bianchini, B. Casal, G. Dissertori, M. Dittmar, M. Donegà, C. Grab, C. Heidegger, D. Hits, J. Hoss, G. Kasieczka, T. Klijnsma, W. Lustermann, B. Mangano, M. Marionneau, M.T. Meinhard, D. Meister, F. Micheli, P. Musella, F. Nessi-Tedaldi, F. Pandolfi, J. Pata, F. Pauss, G. Perrin, L. Perrozzi, M. Quittnat, M. Rossini, M. Schönenberger, L. Shchutska, A. Starodumov[49], V.R. Tavolaro, K. Theofilatos, M.L. Vesterbacka Olsson, R. Wallny, A. Zagozdzinska[35], D.H. Zhu

Universität Zürich, Zurich, Switzerland
T.K. Aarrestad, C. Amsler[50], L. Caminada, M.F. Canelli, A. De Cosa, S. Donato, C. Galloni, A. Hinzmann, T. Hreus, B. Kilminster, J. Ngadiuba, D. Pinna, G. Rauco, P. Robmann, D. Salerno, C. Seitz, A. Zucchetta

National Central University, Chung-Li, Taiwan
V. Candelise, T.H. Doan, Sh. Jain, R. Khurana, M. Konyushikhin, C.M. Kuo, W. Lin, A. Pozdnyakov, S.S. Yu

National Taiwan University (NTU), Taipei, Taiwan
P. Chang, Y. Chao, K.F. Chen, P.H. Chen, F. Fiori, W.-S. Hou, Y. Hsiung, Arun Kumar, Y.F. Liu, R.-S. Lu, M. Miñano Moya, E. Paganis, A. Psallidas, J.f. Tsai

Chulalongkorn University, Faculty of Science, Department of Physics, Bangkok, Thailand
B. Asavapibhop, K. Kovitanggoon, G. Singh, N. Srimanobhas

Çukurova University, Physics Department, Science and Art Faculty, Adana, Turkey
A. Adiguzel[51], M.N. Bakirci[52], F. Boran, S. Damarseckin, Z.S. Demiroglu, C. Dozen, E. Eskut, S. Girgis, G. Gokbulut, Y. Guler, I. Hos[53], E.E. Kangal[54], O. Kara, U. Kiminsu, M. Oglakci, G. Onengut[55], K. Ozdemir[56], S. Ozturk[52], A. Polatoz, D. Sunar Cerci[57], S. Turkcapar, I.S. Zorbakir, C. Zorbilmez

Middle East Technical University, Physics Department, Ankara, Turkey
B. Bilin, G. Karapinar[58], K. Ocalan[59], M. Yalvac, M. Zeyrek

Bogazici University, Istanbul, Turkey
E. Gülmez, M. Kaya[60], O. Kaya[61], S. Tekten, E.A. Yetkin[62]

Istanbul Technical University, Istanbul, Turkey
M.N. Agaras, S. Atay, A. Cakir, K. Cankocak

Institute for Scintillation Materials of National Academy of Science of Ukraine, Kharkov, Ukraine
B. Grynyov

National Scientific Center, Kharkov Institute of Physics and Technology, Kharkov, Ukraine
L. Levchuk, P. Sorokin

University of Bristol, Bristol, United Kingdom
R. Aggleton, F. Ball, L. Beck, J.J. Brooke, D. Burns, E. Clement, D. Cussans, H. Flacher, J. Goldstein, M. Grimes, G.P. Heath, H.F. Heath, J. Jacob, L. Kreczko, C. Lucas, D.M. Newbold[63], S. Paramesvaran, A. Poll, T. Sakuma, S. Seif El Nasr-storey, D. Smith, V.J. Smith

Rutherford Appleton Laboratory, Didcot, United Kingdom
A. Belyaev[64], C. Brew, R.M. Brown, L. Calligaris, D. Cieri, D.J.A. Cockerill, J.A. Coughlan, K. Harder, S. Harper, E. Olaiya, D. Petyt, C.H. Shepherd-Themistocleous, A. Thea, I.R. Tomalin, T. Williams

Imperial College, London, United Kingdom
M. Baber, R. Bainbridge, S. Breeze, O. Buchmuller, A. Bundock, S. Casasso, M. Citron, D. Colling, L. Corpe, P. Dauncey, G. Davies, A. De Wit, M. Della Negra, R. Di Maria, P. Dunne, A. Elwood, D. Futyan, Y. Haddad, G. Hall, G. Iles, T. James, R. Lane, C. Laner, L. Lyons, A.-M. Magnan, S. Malik, L. Mastrolorenzo, T. Matsushita, J. Nash, A. Nikitenko[49], J. Pela, M. Pesaresi, D.M. Raymond, A. Richards, A. Rose, E. Scott, C. Seez, A. Shtipliyski, S. Summers, A. Tapper, K. Uchida, M. Vazquez Acosta[65], T. Virdee[14], D. Winterbottom, J. Wright, S.C. Zenz

Brunel University, Uxbridge, United Kingdom
J.E. Cole, P.R. Hobson, A. Khan, P. Kyberd, I.D. Reid, P. Symonds, L. Teodorescu, M. Turner

Baylor University, Waco, USA
A. Borzou, K. Call, J. Dittmann, K. Hatakeyama, H. Liu, N. Pastika

Catholic University of America, Washington DC, USA
R. Bartek, A. Dominguez

The University of Alabama, Tuscaloosa, USA
A. Buccilli, S.I. Cooper, C. Henderson, P. Rumerio, C. West

Boston University, Boston, USA
D. Arcaro, A. Avetisyan, T. Bose, D. Gastler, D. Rankin, C. Richardson, J. Rohlf, L. Sulak, D. Zou

Brown University, Providence, USA
G. Benelli, D. Cutts, A. Garabedian, J. Hakala, U. Heintz, J.M. Hogan, K.H.M. Kwok, E. Laird, G. Landsberg, Z. Mao, M. Narain, J. Pazzini, S. Piperov, S. Sagir, R. Syarif, D. Yu

University of California, Davis, Davis, USA
R. Band, C. Brainerd, D. Burns, M. Calderon De La Barca Sanchez, M. Chertok, J. Conway, R. Conway, P.T. Cox, R. Erbacher, C. Flores, G. Funk, M. Gardner, W. Ko, R. Lander, C. Mclean, M. Mulhearn, D. Pellett, J. Pilot, S. Shalhout, M. Shi, J. Smith, M. Squires, D. Stolp, K. Tos, M. Tripathi, Z. Wang

University of California, Los Angeles, USA
M. Bachtis, C. Bravo, R. Cousins, A. Dasgupta, A. Florent, J. Hauser, M. Ignatenko, N. Mccoll, D. Saltzberg, C. Schnaible, V. Valuev

University of California, Riverside, Riverside, USA
E. Bouvier, K. Burt, R. Clare, J. Ellison, J.W. Gary, S.M.A. Ghiasi Shirazi, G. Hanson, J. Heilman, P. Jandir, E. Kennedy, F. Lacroix, O.R. Long, M. Olmedo Negrete, M.I. Paneva, A. Shrinivas, W. Si, H. Wei, S. Wimpenny, B. R. Yates

University of California, San Diego, La Jolla, USA
J.G. Branson, G.B. Cerati, S. Cittolin, M. Derdzinski, R. Gerosa, B. Hashemi, A. Holzner, D. Klein, G. Kole, V. Krutelyov, J. Letts, I. Macneill, M. Masciovecchio, D. Olivito, S. Padhi, M. Pieri, M. Sani, V. Sharma, S. Simon, M. Tadel, A. Vartak, S. Wasserbaech[66], J. Wood, F. Würthwein, A. Yagil, G. Zevi Della Porta

University of California, Santa Barbara - Department of Physics, Santa Barbara, USA
N. Amin, R. Bhandari, J. Bradmiller-Feld, C. Campagnari, A. Dishaw, V. Dutta, M. Franco Sevilla, C. George, F. Golf, L. Gouskos, J. Gran, R. Heller, J. Incandela, S.D. Mullin, A. Ovcharova, H. Qu, J. Richman, D. Stuart, I. Suarez, J. Yoo

California Institute of Technology, Pasadena, USA
D. Anderson, J. Bendavid, A. Bornheim, J.M. Lawhorn, H.B. Newman, T. Nguyen, C. Pena, M. Spiropulu, J.R. Vlimant, S. Xie, Z. Zhang, R.Y. Zhu

Carnegie Mellon University, Pittsburgh, USA
M.B. Andrews, T. Ferguson, T. Mudholkar, M. Paulini, J. Russ, M. Sun, H. Vogel, I. Vorobiev, M. Weinberg

University of Colorado Boulder, Boulder, USA
J.P. Cumalat, W.T. Ford, F. Jensen, A. Johnson, M. Krohn, S. Leontsinis, T. Mulholland, K. Stenson, S.R. Wagner

Cornell University, Ithaca, USA
J. Alexander, J. Chaves, J. Chu, S. Dittmer, K. Mcdermott, N. Mirman, J.R. Patterson, A. Rinkevicius, A. Ryd, L. Skinnari, L. Soffi, S.M. Tan, Z. Tao, J. Thom, J. Tucker, P. Wittich, M. Zientek

Fermi National Accelerator Laboratory, Batavia, USA
S. Abdullin, M. Albrow, G. Apollinari, A. Apresyan, A. Apyan, S. Banerjee, L.A.T. Bauerdick, A. Beretvas, J. Berryhill, P.C. Bhat, G. Bolla, K. Burkett, J.N. Butler, A. Canepa, H.W.K. Cheung, F. Chlebana, M. Cremonesi, J. Duarte, V.D. Elvira, J. Freeman, Z. Gecse, E. Gottschalk, L. Gray, D. Green, S. Grünendahl, O. Gutsche, R.M. Harris, S. Hasegawa, J. Hirschauer, Z. Hu, B. Jayatilaka, S. Jindariani, M. Johnson, U. Joshi, B. Klima, B. Kreis, S. Lammel, D. Lincoln, R. Lipton, M. Liu, T. Liu, R. Lopes De Sá, J. Lykken, K. Maeshima, N. Magini, J.M. Marraffino, S. Maruyama, D. Mason, P. McBride, P. Merkel, S. Mrenna, S. Nahn, V. O'Dell, K. Pedro, O. Prokofyev, G. Rakness, L. Ristori, B. Schneider, E. Sexton-Kennedy, A. Soha, W.J. Spalding, L. Spiegel, S. Stoynev, J. Strait, N. Strobbe, L. Taylor, S. Tkaczyk, N.V. Tran, L. Uplegger, E.W. Vaandering, C. Vernieri, M. Verzocchi, R. Vidal, M. Wang, H.A. Weber, A. Whitbeck

University of Florida, Gainesville, USA
D. Acosta, P. Avery, P. Bortignon, A. Brinkerhoff, A. Carnes, M. Carver, D. Curry, S. Das, R.D. Field, I.K. Furic, J. Konigsberg, A. Korytov, K. Kotov, P. Ma, K. Matchev, H. Mei, G. Mitselmakher, D. Rank, D. Sperka, N. Terentyev, L. Thomas, J. Wang, S. Wang, J. Yelton

Florida International University, Miami, USA
Y.R. Joshi, S. Linn, P. Markowitz, G. Martinez, J.L. Rodriguez

Florida State University, Tallahassee, USA
A. Ackert, T. Adams, A. Askew, S. Hagopian, V. Hagopian, K.F. Johnson, T. Kolberg, T. Perry, H. Prosper, A. Santra, R. Yohay

Florida Institute of Technology, Melbourne, USA
M.M. Baarmand, V. Bhopatkar, S. Colafranceschi, M. Hohlmann, D. Noonan, T. Roy, F. Yumiceva

University of Illinois at Chicago (UIC), Chicago, USA
M.R. Adams, L. Apanasevich, D. Berry, R.R. Betts, R. Cavanaugh, X. Chen, O. Evdokimov, C.E. Gerber, D.A. Hangal, D.J. Hofman, K. Jung, J. Kamin, I.D. Sandoval Gonzalez, M.B. Tonjes, H. Trauger, N. Varelas, H. Wang, Z. Wu, J. Zhang

The University of Iowa, Iowa City, USA
B. Bilki[67], W. Clarida, K. Dilsiz[68], S. Durgut, R.P. Gandrajula, M. Haytmyradov, V. Khristenko, J.-P. Merlo, H. Mermerkaya[69], A. Mestvirishvili, A. Moeller, J. Nachtman, H. Ogul[70], Y. Onel, F. Ozok[71], A. Penzo, C. Snyder, E. Tiras, J. Wetzel, K. Yi

Johns Hopkins University, Baltimore, USA
B. Blumenfeld, A. Cocoros, N. Eminizer, D. Fehling, L. Feng, A.V. Gritsan, P. Maksimovic, J. Roskes, U. Sarica, M. Swartz, M. Xiao, C. You

The University of Kansas, Lawrence, USA
A. Al-bataineh, P. Baringer, A. Bean, S. Boren, J. Bowen, J. Castle, S. Khalil, A. Kropivnitskaya, D. Majumder, W. Mcbrayer, M. Murray, C. Royon, S. Sanders, E. Schmitz, R. Stringer, J.D. Tapia Takaki, Q. Wang

Kansas State University, Manhattan, USA
A. Ivanov, K. Kaadze, Y. Maravin, A. Mohammadi, L.K. Saini, N. Skhirtladze, S. Toda

Lawrence Livermore National Laboratory, Livermore, USA
F. Rebassoo, D. Wright

University of Maryland, College Park, USA
C. Anelli, A. Baden, O. Baron, A. Belloni, B. Calvert, S.C. Eno, C. Ferraioli, N.J. Hadley,

S. Jabeen, G.Y. Jeng, R.G. Kellogg, J. Kunkle, A.C. Mignerey, F. Ricci-Tam, Y.H. Shin, A. Skuja, S.C. Tonwar

Massachusetts Institute of Technology, Cambridge, USA
D. Abercrombie, B. Allen, V. Azzolini, R. Barbieri, A. Baty, R. Bi, S. Brandt, W. Busza, I.A. Cali, M. D'Alfonso, Z. Demiragli, G. Gomez Ceballos, M. Goncharov, D. Hsu, Y. Iiyama, G.M. Innocenti, M. Klute, D. Kovalskyi, Y.S. Lai, Y.-J. Lee, A. Levin, P.D. Luckey, B. Maier, A.C. Marini, C. Mcginn, C. Mironov, S. Narayanan, X. Niu, C. Paus, C. Roland, G. Roland, J. Salfeld-Nebgen, G.S.F. Stephans, K. Tatar, D. Velicanu, J. Wang, T.W. Wang, B. Wyslouch

University of Minnesota, Minneapolis, USA
A.C. Benvenuti, R.M. Chatterjee, A. Evans, P. Hansen, S. Kalafut, S.C. Kao, Y. Kubota, Z. Lesko, J. Mans, S. Nourbakhsh, N. Ruckstuhl, R. Rusack, N. Tambe, J. Turkewitz

University of Mississippi, Oxford, USA
J.G. Acosta, S. Oliveros

University of Nebraska-Lincoln, Lincoln, USA
E. Avdeeva, K. Bloom, D.R. Claes, C. Fangmeier, R. Gonzalez Suarez, R. Kamalieddin, I. Kravchenko, J. Monroy, J.E. Siado, G.R. Snow, B. Stieger

State University of New York at Buffalo, Buffalo, USA
M. Alyari, J. Dolen, A. Godshalk, C. Harrington, I. Iashvili, D. Nguyen, A. Parker, S. Rappoccio, B. Roozbahani

Northeastern University, Boston, USA
G. Alverson, E. Barberis, A. Hortiangtham, A. Massironi, D.M. Morse, D. Nash, T. Orimoto, R. Teixeira De Lima, D. Trocino, R.-J. Wang, D. Wood

Northwestern University, Evanston, USA
S. Bhattacharya, O. Charaf, K.A. Hahn, N. Mucia, N. Odell, B. Pollack, M.H. Schmitt, K. Sung, M. Trovato, M. Velasco

University of Notre Dame, Notre Dame, USA
N. Dev, M. Hildreth, K. Hurtado Anampa, C. Jessop, D.J. Karmgard, N. Kellams, K. Lannon, N. Loukas, N. Marinelli, F. Meng, C. Mueller, Y. Musienko[36], M. Planer, A. Reinsvold, R. Ruchti, G. Smith, S. Taroni, M. Wayne, M. Wolf, A. Woodard

The Ohio State University, Columbus, USA
J. Alimena, L. Antonelli, B. Bylsma, L.S. Durkin, S. Flowers, B. Francis, A. Hart, C. Hill, W. Ji, B. Liu, W. Luo, D. Puigh, B.L. Winer, H.W. Wulsin

Princeton University, Princeton, USA
A. Benaglia, S. Cooperstein, O. Driga, P. Elmer, J. Hardenbrook, P. Hebda, D. Lange, J. Luo, D. Marlow, K. Mei, I. Ojalvo, J. Olsen, C. Palmer, P. Piroué, D. Stickland, A. Svyatkovskiy, C. Tully

University of Puerto Rico, Mayaguez, USA
S. Malik, S. Norberg

Purdue University, West Lafayette, USA
A. Barker, V.E. Barnes, S. Folgueras, L. Gutay, M.K. Jha, M. Jones, A.W. Jung, A. Khatiwada, D.H. Miller, N. Neumeister, J.F. Schulte, J. Sun, F. Wang, W. Xie

Purdue University Northwest, Hammond, USA
T. Cheng, N. Parashar, J. Stupak

Rice University, Houston, USA
A. Adair, B. Akgun, Z. Chen, K.M. Ecklund, F.J.M. Geurts, M. Guilbaud, W. Li, B. Michlin, M. Northup, B.P. Padley, J. Roberts, J. Rorie, Z. Tu, J. Zabel

University of Rochester, Rochester, USA
A. Bodek, P. de Barbaro, R. Demina, Y.t. Duh, T. Ferbel, M. Galanti, A. Garcia-Bellido, J. Han, O. Hindrichs, A. Khukhunaishvili, K.H. Lo, P. Tan, M. Verzetti

The Rockefeller University, New York, USA
R. Ciesielski, K. Goulianos, C. Mesropian

Rutgers, The State University of New Jersey, Piscataway, USA
A. Agapitos, J.P. Chou, Y. Gershtein, T.A. Gómez Espinosa, E. Halkiadakis, M. Heindl, E. Hughes, S. Kaplan, R. Kunnawalkam Elayavalli, S. Kyriacou, A. Lath, R. Montalvo, K. Nash, M. Osherson, H. Saka, S. Salur, S. Schnetzer, D. Sheffield, S. Somalwar, R. Stone, S. Thomas, P. Thomassen, M. Walker

University of Tennessee, Knoxville, USA
M. Foerster, J. Heideman, G. Riley, K. Rose, S. Spanier, K. Thapa

Texas A&M University, College Station, USA
O. Bouhali[72], A. Castaneda Hernandez[72], A. Celik, M. Dalchenko, M. De Mattia, A. Delgado, S. Dildick, R. Eusebi, J. Gilmore, T. Huang, T. Kamon[73], R. Mueller, Y. Pakhotin, R. Patel, A. Perloff, L. Perniè, D. Rathjens, A. Safonov, A. Tatarinov, K.A. Ulmer

Texas Tech University, Lubbock, USA
N. Akchurin, J. Damgov, F. De Guio, P.R. Dudero, J. Faulkner, E. Gurpinar, S. Kunori, K. Lamichhane, S.W. Lee, T. Libeiro, T. Peltola, S. Undleeb, I. Volobouev, Z. Wang

Vanderbilt University, Nashville, USA
S. Greene, A. Gurrola, R. Janjam, W. Johns, C. Maguire, A. Melo, H. Ni, P. Sheldon, S. Tuo, J. Velkovska, Q. Xu

University of Virginia, Charlottesville, USA
M.W. Arenton, P. Barria, B. Cox, R. Hirosky, A. Ledovskoy, H. Li, C. Neu, T. Sinthuprasith, X. Sun, Y. Wang, E. Wolfe, F. Xia

Wayne State University, Detroit, USA
C. Clarke, R. Harr, P.E. Karchin, J. Sturdy, S. Zaleski

University of Wisconsin - Madison, Madison, WI, USA
D.A. Belknap, J. Buchanan, C. Caillol, S. Dasu, L. Dodd, S. Duric, B. Gomber, M. Grothe, M. Herndon, A. Hervé, U. Hussain, P. Klabbers, A. Lanaro, A. Levine, K. Long, R. Loveless, G.A. Pierro, G. Polese, T. Ruggles, A. Savin, N. Smith, W.H. Smith, D. Taylor, N. Woods

†: Deceased
1: Also at Vienna University of Technology, Vienna, Austria
2: Also at State Key Laboratory of Nuclear Physics and Technology; Peking University, Beijing, China
3: Also at Universidade Estadual de Campinas, Campinas, Brazil
4: Also at Universidade Federal de Pelotas, Pelotas, Brazil
5: Also at Université Libre de Bruxelles, Bruxelles, Belgium
6: Also at Joint Institute for Nuclear Research, Dubna, Russia
7: Also at Helwan University, Cairo, Egypt
8: Now at Zewail City of Science and Technology, Zewail, Egypt

9: Also at Fayoum University, El-Fayoum, Egypt
10: Now at British University in Egypt, Cairo, Egypt
11: Also at Université de Haute Alsace, Mulhouse, France
12: Also at Skobeltsyn Institute of Nuclear Physics; Lomonosov Moscow State University, Moscow, Russia
13: Also at Tbilisi State University, Tbilisi, Georgia
14: Also at CERN; European Organization for Nuclear Research, Geneva, Switzerland
15: Also at RWTH Aachen University; III. Physikalisches Institut A, Aachen, Germany
16: Also at University of Hamburg, Hamburg, Germany
17: Also at Brandenburg University of Technology, Cottbus, Germany
18: Also at Institute of Nuclear Research ATOMKI, Debrecen, Hungary
19: Also at MTA-ELTE Lendület CMS Particle and Nuclear Physics Group; Eötvös Loránd University, Budapest, Hungary
20: Also at Institute of Physics; University of Debrecen, Debrecen, Hungary
21: Also at Indian Institute of Technology Bhubaneswar, Bhubaneswar, India
22: Also at Institute of Physics, Bhubaneswar, India
23: Also at University of Visva-Bharati, Santiniketan, India
24: Also at University of Ruhuna, Matara, Sri Lanka
25: Also at Isfahan University of Technology, Isfahan, Iran
26: Also at Yazd University, Yazd, Iran
27: Also at Plasma Physics Research Center; Science and Research Branch; Islamic Azad University, Tehran, Iran
28: Also at Università degli Studi di Siena, Siena, Italy
29: Also at INFN Sezione di Milano-Bicocca; Università di Milano-Bicocca, Milano, Italy
30: Also at Laboratori Nazionali di Legnaro dell'INFN, Legnaro, Italy
31: Also at Purdue University, West Lafayette, USA
32: Also at International Islamic University of Malaysia, Kuala Lumpur, Malaysia
33: Also at Malaysian Nuclear Agency; MOSTI, Kajang, Malaysia
34: Also at Consejo Nacional de Ciencia y Tecnología, Mexico city, Mexico
35: Also at Warsaw University of Technology; Institute of Electronic Systems, Warsaw, Poland
36: Also at Institute for Nuclear Research, Moscow, Russia
37: Now at National Research Nuclear University 'Moscow Engineering Physics Institute' (MEPhI), Moscow, Russia
38: Also at St. Petersburg State Polytechnical University, St. Petersburg, Russia
39: Also at University of Florida, Gainesville, USA
40: Also at P.N. Lebedev Physical Institute, Moscow, Russia
41: Also at INFN Sezione di Padova; Università di Padova; Università di Trento (Trento), Padova, Italy
42: Also at Budker Institute of Nuclear Physics, Novosibirsk, Russia
43: Also at Faculty of Physics; University of Belgrade, Belgrade, Serbia
44: Also at INFN Sezione di Roma; Sapienza Università di Roma, Rome, Italy
45: Also at University of Belgrade; Faculty of Physics and Vinca Institute of Nuclear Sciences, Belgrade, Serbia
46: Also at Scuola Normale e Sezione dell'INFN, Pisa, Italy
47: Also at National and Kapodistrian University of Athens, Athens, Greece
48: Also at Riga Technical University, Riga, Latvia
49: Also at Institute for Theoretical and Experimental Physics, Moscow, Russia
50: Also at Albert Einstein Center for Fundamental Physics, Bern, Switzerland
51: Also at Istanbul University; Faculty of Science, Istanbul, Turkey

52: Also at Gaziosmanpasa University, Tokat, Turkey
53: Also at Istanbul Aydin University, Istanbul, Turkey
54: Also at Mersin University, Mersin, Turkey
55: Also at Cag University, Mersin, Turkey
56: Also at Piri Reis University, Istanbul, Turkey
57: Also at Adiyaman University, Adiyaman, Turkey
58: Also at Izmir Institute of Technology, Izmir, Turkey
59: Also at Necmettin Erbakan University, Konya, Turkey
60: Also at Marmara University, Istanbul, Turkey
61: Also at Kafkas University, Kars, Turkey
62: Also at Istanbul Bilgi University, Istanbul, Turkey
63: Also at Rutherford Appleton Laboratory, Didcot, United Kingdom
64: Also at School of Physics and Astronomy; University of Southampton, Southampton, United Kingdom
65: Also at Instituto de Astrofísica de Canarias, La Laguna, Spain
66: Also at Utah Valley University, Orem, USA
67: Also at Beykent University, Istanbul, Turkey
68: Also at Bingol University, Bingol, Turkey
69: Also at Erzincan University, Erzincan, Turkey
70: Also at Sinop University, Sinop, Turkey
71: Also at Mimar Sinan University; Istanbul, Istanbul, Turkey
72: Also at Texas A&M University at Qatar, Doha, Qatar
73: Also at Kyungpook National University, Daegu, Korea